

WL-TR-91-4090

AD-A259 203

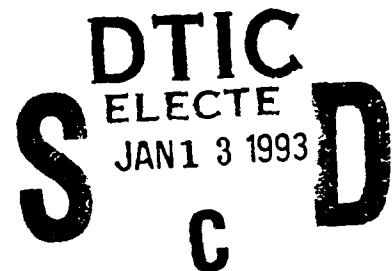


2

**COMPRESSION AFTER IMPACT
BEHAVIOR OF ARALL®-1
LAMINATES**



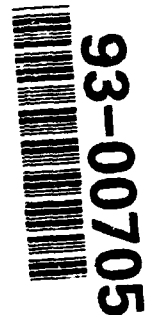
**WILLIAM P. HOOGSTEDEN
MATERIALS BEHAVIOR & EVALUATION GROUP
MATERIALS ENGINEERING BRANCH
SYSTEMS SUPPORT DIVISION**



JULY 1992

**FINAL TECHNICAL REPORT FOR PERIOD
JUNE 1987- NOVEMBER 1987**

APPROVED FOR PUBLIC RELEASE; DISTRIBUTION UNLIMITED



**MATERIALS DIRECTORATE
WRIGHT LABORATORY
AIR FORCE SYSTEMS COMMAND
WRIGHT-PATTERSON AFB, OHIO 45433-6533**

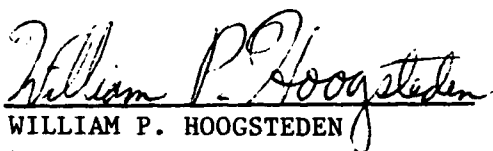
93 1 12 001

NOTICE

When Government drawings, specifications, or other data are used for any purpose other than in connection with a definitely Government-related procurement, the United States Government incurs no responsibility nor any obligation whatsoever. The fact that the government may have formulated, or in any way supplied the said drawings, specifications, or other data, is not to be regarded by implication or otherwise in any manner construed, as licensing the holder or any other person or corporation, or as conveying any rights or permission to manufacture, use, or sell any patented invention that may in any way be related thereto.

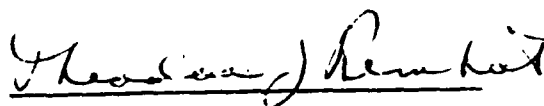
This report is releasable to the National Technical Information Service (NTIS). At NTIS, it will be available to the general public, including foreign nations.

This technical report has been reviewed and is approved for publication.

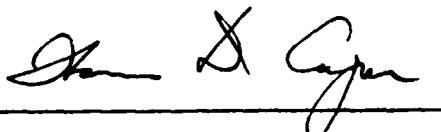


WILLIAM P. HOOGSTEDEN
Materials Engineer
Materials Behavior & Evaluation Group
Materials Engineering Branch

FOR THE COMMANDER



THEODORE J. REINHART, Chief
Materials Engineering Branch
Systems Support Division



THOMAS D. COOPER, Chief
Systems Support Division
Materials Directorate

If your address has changed, if you wish to be removed from our mailing list, or if the addressee is no longer employed by your organization, please notify WL/MLSE, Wright-Patterson AFB, OH 45433-6533 to help us maintain a current mailing list.

Copies of this report should not be returned unless return is required by security considerations, contractual obligations, or notice on a specific document.

REPORT DOCUMENTATION PAGE			Form Approved OMB No. 0704-0188	
<small>Public reporting burden for this collection of information is estimated to average 1 hour per response, including the time for reviewing instructions, searching existing data sources, gathering and maintaining the data needed, and completing and reviewing the collection of information. Send comments regarding this burden estimate or any other aspect of this collection of information, including suggestions for reducing this burden, to Washington Headquarters Services, Directorate for Information Operations and Reports, 1215 Jefferson Davis Highway, Suite 1204, Arlington, VA 22202-4302, and to the Office of Management and Budget, Paperwork Reduction Project (0704-0188), Washington, DC 20503.</small>				
1. AGENCY USE ONLY (Leave blank)		2. REPORT DATE 14 Jul 92		3. REPORT TYPE AND DATES COVERED FINAL REPORT, JUN 87 TO NOV
4. TITLE AND SUBTITLE COMPRESSION-AFTER-IMPACT BEHAVIOR OF ARRALL®-1 LAMINATES			5. FUNDING NUMBERS PE 62102F PR 2418 TA 07 WU 03	
6. AUTHOR(S) HOOGSTEDEN WILLIAM				
7. PERFORMING ORGANIZATION NAME(S) AND ADDRESS(ES) Materials Behavior & Evaluation Group Materials Engineering Branch Systems Support Division Materials Directorate (WL/MLSE) Wright Patterson AFB OH 45433-6533			8. PERFORMING ORGANIZATION REPORT NUMBER WL-TR-91-4090	
9. SPONSORING / MONITORING AGENCY NAME(S) AND ADDRESS(ES)			10. SPONSORING / MONITORING AGENCY REPORT NUMBER	
11. SUPPLEMENTARY NOTES				
12a. DISTRIBUTION / AVAILABILITY STATEMENT APPROVED FOR PUBLIC RELEASE DISTRIBUTION UNLIMITED			12b. DISTRIBUTION CODE	
13. ABSTRACT (Maximum 200 words) <p>ARALL® laminates are the first generation of a new class of materials combining the best properties of metals and composite materials. This report represents part of a Phase I of a two phase study of ARALL® -1 laminates.</p> <p>Ten specimens were tested in a modified Boeing Compression-After-Impact fixture. Two specimens were undamaged. The remaining eight received impacts of 2.3 ft-lbs (3.18J), 5.5 ft-lbs (7.5J), 10.4 ft-lbs (14.1J), and 11.7 ft-lbs (15.9J). Only dents were produced at 2.3 ft-lbs (3.18J). Back face cracks appeared at 5.5 ft-lbs (7.5J). Full penetration was achieved at 10.4 ft-lbs (14.1J). Interior damage as measured by ultrasonic "C" scan showed little damage beyond that already visible on the surface.</p> <p>Compressive buckling was the mode of failure. Increasing impact energy decreased the buckling load of the specimens. "C" scans taken after compression testing revealed no growth of the interior damage.</p>				
14. SUBJECT TERMS			15. NUMBER OF PAGES 52	
			16. PRICE CODE	
17. SECURITY CLASSIFICATION OF REPORT UNCLASSIFIED	18. SECURITY CLASSIFICATION OF THIS PAGE UNCLASSIFIED	19. SECURITY CLASSIFICATION OF ABSTRACT UNCLASSIFIED	20. LIMITATION OF ABSTRACT UL	

TABLE OF CONTENTS

TABLE OF CONTENTS	iii
LIST OF FIGURES	iv
LIST OF TABLES	vi
1. INTRODUCTION	1
2. MATERIALS AND SPECIMENS	2
3. TEST PROCEDURES	4
3.1. IMPACT TESTING	4
3.2. COMPRESSION TESTING	6
4. TEST RESULTS AND DISCUSSION	8
4.1. IMPACT RESULTS	8
4.2. COMPRESSION RESULTS	18
5. CONCLUSIONS	28
6. RECOMMENDATIONS	29
7. REFERENCES	30
A. Appendix	31
A.1. Specimen Photographs	31
A.2. "C" Scans of Damage Areas	39

QUALITY INSPECTED 1

Accession For	
NTIS GRA&I	<input checked="checked" type="checkbox"/>
DTIC TAB	<input type="checkbox"/>
Unannounced	<input type="checkbox"/>
Justification	
By	
Distribution/	
Availability Codes	
Avail and/or	
Dist	Special
A-1	

LIST OF FIGURES

2-1: Schematic Lay-up of ARALL®-1.....	2
2-2: The Modified Compression After Impact Specimen.....	3
3-1: Schematic of the Impact Test Apparatus.....	5
3-2: Specimen Strain Gauge Positions.....	6
3-3: The Modified Boeing Compression After Impact Fixture.....	7
4-1: Force and Energy vs. Time Plot for Specimen A3.....	9
4-2: Force and Energy vs. Time Plots for Specimen A4.....	9
4-3: Force and Energy vs. Time for Specimen A5.....	10
4-4: Force and Energy vs. Time for Specimen A6.....	11
4-5: Force vs. Calculated Displacement for Specimen A5.....	12
4-6: Force vs. Calculated Displacement for Specimen A6.....	12
4-7: Force and Energy vs. Time for Specimen A7.....	14
4-8: Force and Energy vs. Time for Specimen A8.....	14
4-9: Force and Energy vs. Time for Specimen A9.....	15
4-10: Force and Energy vs. Time for Specimen A10.....	15
4-11: Energy Absorbed vs. Impact Energy.....	16
4-12: Energy Absorbed vs. Normalized Impact Energy.....	17
4-13: Normalized Damage Area vs. Normalized Impact Energy.....	18
4-14: Stress-Strain Curves for Specimen A1.....	20
4-15: Stress-Strain Curves for Specimen A2.....	20
4-16: Stress-Strain Curves for Specimen A3.....	21
4-17: Stress-Strain Curves for Specimen A4.....	21
4-18: Stress-Strain Curves for Specimen A5.....	22
4-19: Stress-Strain Curves for Specimen A6.....	22
4-20: Stress-Strain Curves for Specimen A7.....	23
4-21: Stress-Strain Curves for Specimen A8.....	23
4-22: Stress-Strain Curves for Specimen A9.....	24
4-23: Stress-Strain Curves for Specimen A10.....	24
4-24: Compression After Impact Strength vs. Impact Energy.....	26
A-1: Impact Side of Specimen 3, 2.35 ft-lbs (3.19 J).....	31
A-2: Backface Side of Specimen 3, 2.35 ft-lbs (3.19 J).....	31
A-3: Impact side of Specimen A4, 2.39 ft-lbs (3.23 J).....	32
A-4: Back Side of Specimen A4, 2.29 ft-lbs (3.23 J).....	32
A-5: Impact Side of Specimen A5, 5.54 ft-lbs (7.51 J).....	33
A-6: Back side of Specimen A5, 5.54 ft-lbs (7.51 J).....	33
A-7: Impact Side of Specimen A6, 5.49 ft-lbs (7.44J).....	34
A-8: Backside of Specimen A6, 5.49 ft-lbs (7.44 J).....	34
A-9: Impact Side of Specimen A7, 10.45 ft-lbs (14.2J).....	35
A-10: Back Side of Specimen A7, 10.45 ft-lbs (14.2 J).....	35
A-11: Impact side of Specimen A8, 10.31 ft-lbs (14 J).....	36
A-12: Back Side of Specimen A8, 10.31 ft-lbs (14 J).....	36
A-13: Impact side of Specimen A9, 11.69 ft-lbs (15.8 J).....	37
A-14: Back Side of Specimen A9, 11.69 ft-lbs (15.8 J).....	37
A-15: Impact Side of Specimen A10, 11.7 ft-lbs (15.9 J).....	38
A-16: Back Side of Specimen A10, 11.7 ft-lbs (15.9 J).....	38

LIST OF FIGURES (CONTINUED)

A-17: "C" Scan of Specimen A3, 2.35 ft-lb Impact	39
A-18: "C" Scan of Specimen A3 After Compression Loading	39
A-19: "C" Scan of Specimen A4, 2.39 ft-lb Impact	40
A-20: "C" Scan of Specimen A4 After Compression Loading	40
A-21: "C" Scan of Specimen A5, 5.54 ft-lb Impact	41
A-22: "C" Scan of Specimen A5 After Compression Loading	41
A-23: "C" Scan of Specimen A6, 5.49 ft-lb Impact	42
A-24: "C" Scan of Specimen A6 After Compression Loading	42
A-25: "C" Scan of Specimen A7, 10.45 ft-lb Impact	43
A-26: "C" Scan of Specimen A7 After Compression Loading	43
A-27: "C" Scan of Specimen A8, 10.31 ft-lb Impact	44
A-28: "C" Scan of Specimen A8 After Compression Loading	44
A-29: "C" Scan of Specimen A9, 11.69 ft-lb Impact	45
A-30: "C" Scan of Specimen A9 After Compression Loading	45
A-31: "C" Scan of Specimen A10, 11.7 ft-lb Impact	46
A-32: "C" Scan of Specimen A10 After Compression Loading	46

LIST OF TABLES

4-1: IMPACT DATA.....	18
4-2: INITIAL MODULI FOR UNDAMAGED SPECIMENS.....	19
4-3: COMPRESSION AFTER IMPACT RESULTS.....	27

1. INTRODUCTION

This program is part of the first phase of a two-phase evaluation of ARALL® laminates. This part of the first phase evaluated the effects low velocity impacts have on the compressive properties of ARALL® laminates. ARALL® laminates are a trademark of the ALCOA Corporation.

ARALL® laminates are an attempt to develop a material exploiting the fatigue advantages of composites and the impact and compression advantages of metals. This material is currently made of three layers of aluminum bonded together by two plies of unidirectional aramid fibers in an adhesive matrix. A series of test programs are being run to determine the properties of these ARALL® laminates.

Since ARALL® laminates exhibit characteristics of both composites and metals, both metal and composite tests were conducted on ARALL® laminates during this test program. One of the composite tests was the Compression After Impact test. This test provides a *relative ranking for composite damage tolerance*. It is not a standard test as of this time, but many composite manufacturers and users are using this test to evaluate composite damage tolerance. A description of the test can be found in NASA RP 1142 (Ref. 1).

2. MATERIALS AND SPECIMENS

The specimens tested were the first generation of ARALL® laminates designated ARALL®-1. The ARALL®-1 laminates are three plies of aluminum interleaved with two plies of unidirectional epoxy impregnated aramid fiber as shown in Figure 2-1. ALCOA fabricated the laminates. The aramid fiber is a product of Enka called Twaron®. The aluminum used is 7075. The epoxy resin is a 3M product, AF-163-2.

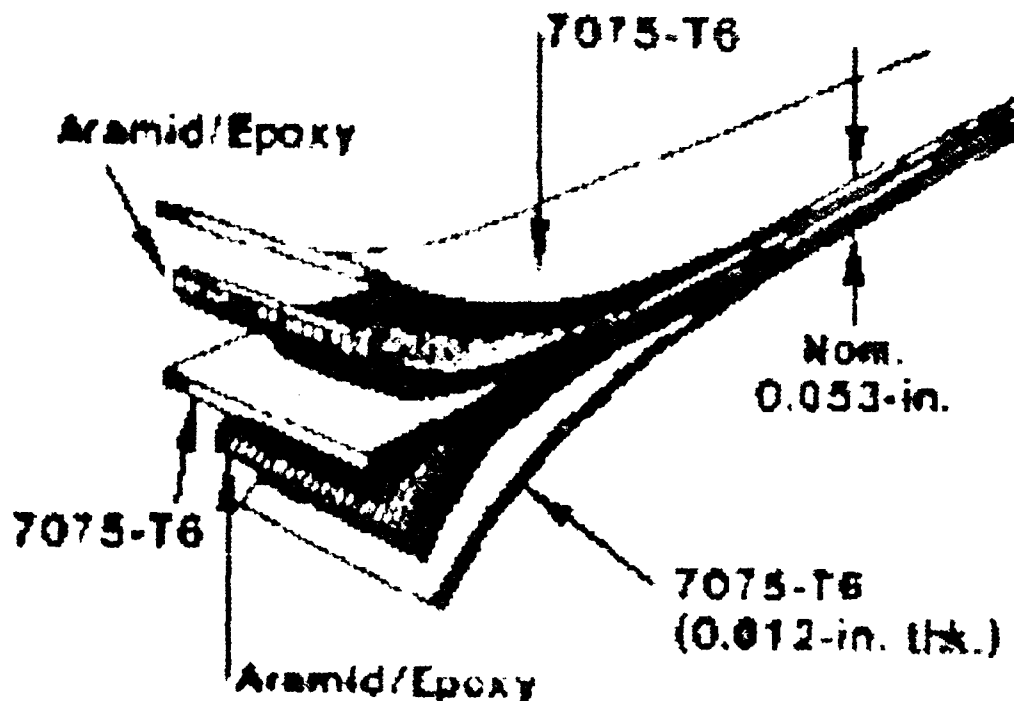


Fig. 2-1: Schematic Lay-up of ARALL®-1.

ALCOA provided 10 specimens which were 10 inches (254 mm) long and 5 inches (127 mm) wide. Figure 2-2 shows the specimens with the impact point and support ring inside diameter noted. The specimens were modified from the NASA RP 1142 (Ref. 1) in that they were fabricated to be 5 inches (127 mm) wide instead of 7 inches (177.8 mm) wide and then machined to 5 inches (127 mm) wide after the impact testing. This saved on machining costs and time between impact and compression testing.

Compression After Impact Specimen ARALL®1

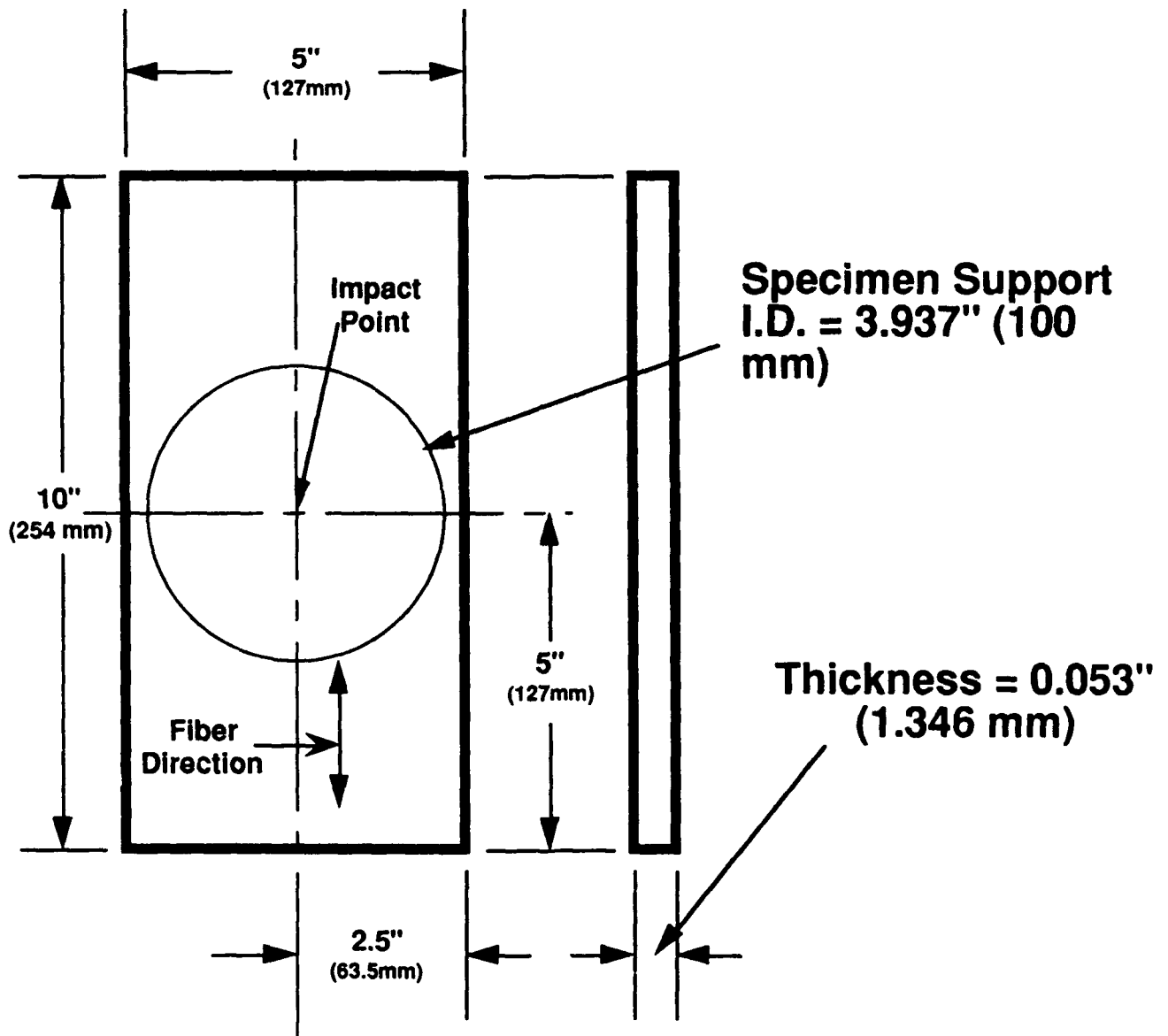


Fig. 2-2: The Modified Compression After Impact Specimen.

3. TEST PROCEDURES

The Compression After Impact (CAI) test is a commonly used test procedure to determine the damage tolerance of composite materials. NASA documented this test as a standard (Ref. 1) as have other materials suppliers and users. Contrary to popular belief, the compression after impact test is actually two tests: an impact test followed by a compression test of the impact damaged specimen. The test gives a relative ranking of how well a material survives an impact.

While previous impact work was done on the impact properties of ARALL[®]-1 laminates at NASA (Ref. 2), this current investigation went further. The NASA work looked only at uninstrumented impact while this work looked at the residual compressive properties of ARALL[®]-1 laminates after impact.

3.1. IMPACT TESTING

A typical Compression After Impact test usually involves an uninstrumented drop tower type impactor and a square clamped support. Reviewing the work of Sjöblom, Reference 3, and Sjöblom, Hartness, and Cordell, Reference 4, indicated more information could be obtained with an instrumented impactor, and the problems involved with secondary impacts could be eliminated by a pendulum impactor. Simple support in a ring geometry would lessen the amount of edge effects and make setup time quicker than the square clamped frame.

Each specimen received an impact from a pendulum type impact apparatus (Figure 3-1). The impact target was located in the center of the specimen 5 inches (127 mm) along the 10 inch (254 mm) dimension and 2.5 inches (63.5 mm) along the 5 inch (127 mm) dimension

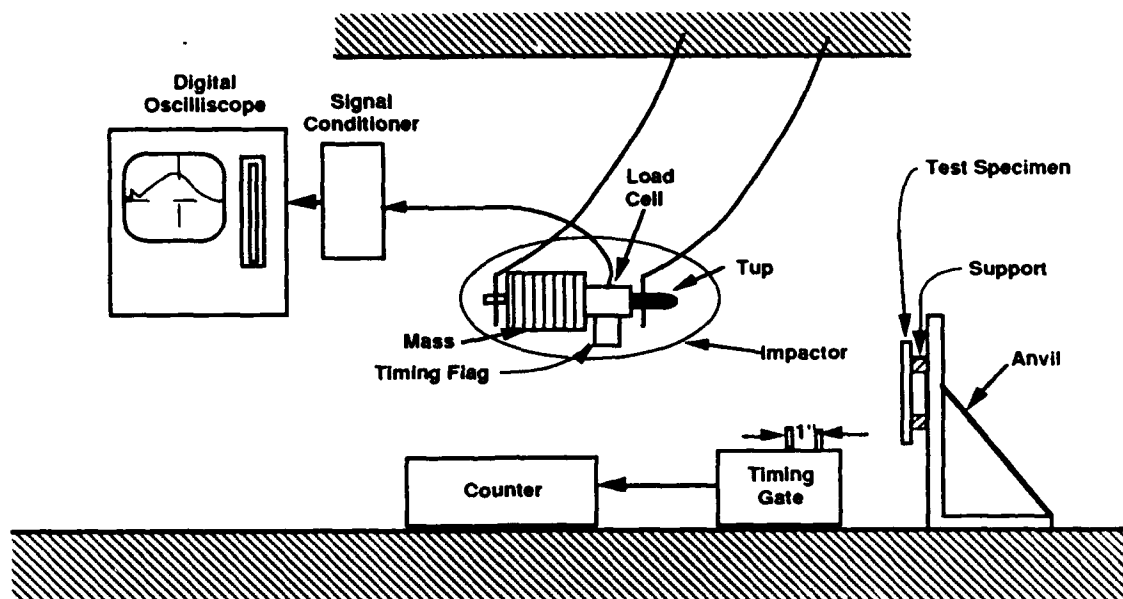


Fig. 3-1: Schematic of the Impact Test Apparatus.

The area impacted was simply supported on a 3.937 inch (100mm) inside diameter ring. The inside diameter of the ring contained a machined radius to minimize edge effects. This type of support was chosen because of the large database available in the Materials Directorate on impacted composite materials using the ring support.

The impactor used was a 1/2-inch (12.7 mm)-diameter hemispherical tup connected to a Dynatup 8496-1 load cell with additional weights so that the total apparatus had a mass of 17.871 pounds (8.987 kg). The load cell is connected to a Nicolet 2090 digital oscilloscope via a Vishay 2310 strain gauge conditioner unit. A timing flag on the impactor triggers photocells 1 inch (25.4 mm) apart for velocity measurement.

A drop height is calculated to achieve the desired impact energy level. Just before impact, the photocell timing gate measures the incoming velocity. While the impactor contacts the specimen, the load cell voltage is recorded by the Nicolet digital oscilloscope as a function of time. When the impactor rebounds, it passes through the timing gate measuring the rebound velocity.

From the digital oscilloscope plot and the incoming and out-going velocities, force vs. time, force vs. displacement, and the energy lost during the impact are calculated. After

the impact, the damage areas were "C"-scanned and compared with "C"-scans taken before the impact to determine the extent of damage. These "C"-scan areas are shown in the odd-numbered Appendix figures A-17 thru A-31. All "C"-scans were done by UTC contractors at the Materials Directorate Systems Support Division facility.

3.2. COMPRESSION TESTING

After the impact testing, each specimen was strain gauged with three pairs of front to back strain gauges (six gauges total). As shown in Figure 3-2, two strain gauge pairs were placed 1 inch (25.4 mm) away from the center of the specimen: one pair directly to the right, and one pair directly to the left of the impact area. The third strain gauge pair went directly above the center of the specimens. All the strain gauges were placed well away from the damaged area.

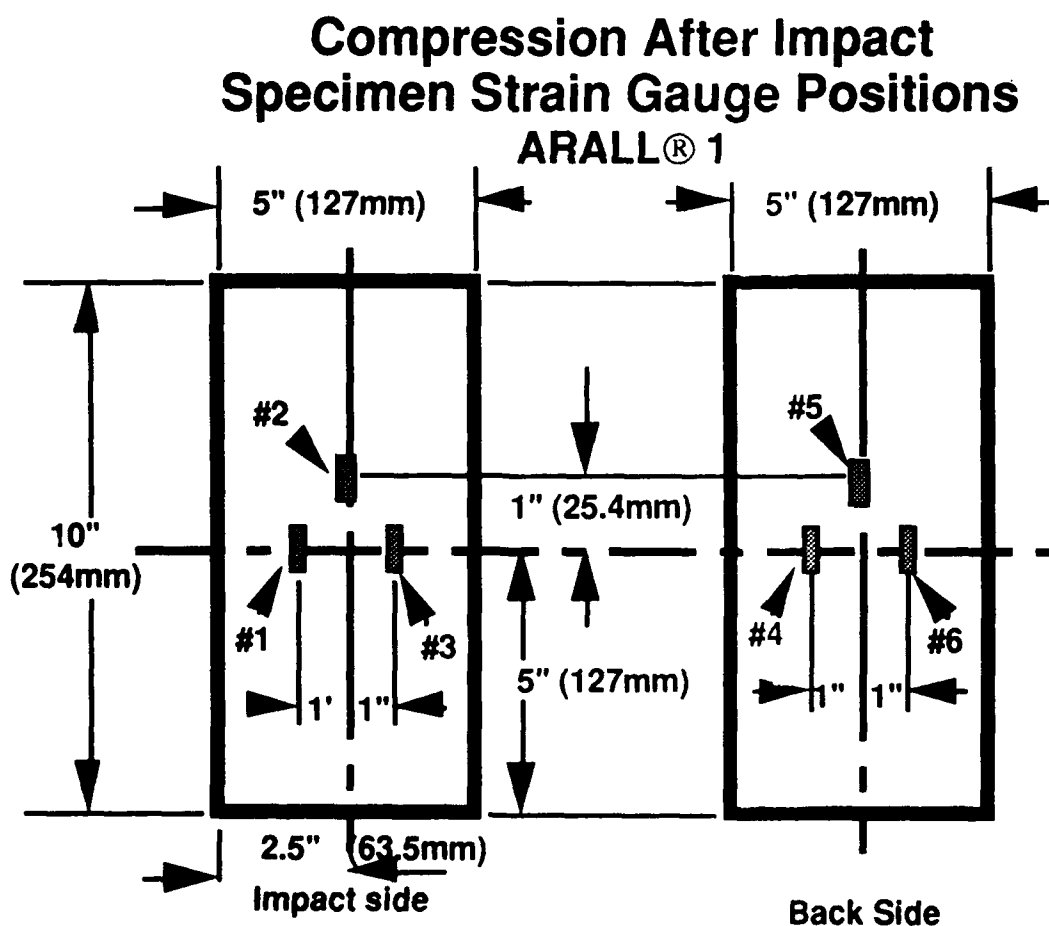


Fig. 3-2: Specimen Strain Gauge Positions.

When strain gauging was completed, each specimen was placed in a modified Boeing Compression Fixture shown in Figure 3-3. This fixture and its modifications are discussed by Manieri and Harmsworth (Ref. 5).

The strain gauges were attached to a Micromeritics MM4000/Hewlett-Packard strain measuring system. The specimen and fixture was aligned and the strains measured by the system during each test.

Each specimen was loaded in a Tinius Olsen Universal test machine. A load rate of 0.05 inch (.127 mm) per minute was used. The load was increased until a continuous drop in load was observed. Loads, strains, and ultimate load were recorded for each test.

After the testing was completed, additional "C"-scans were taken to see if the impact-caused-damage had grown because of the compressive loading. These "C"-scan areas are shown in the even-numbered Appendix figures A-18 thru A-32.

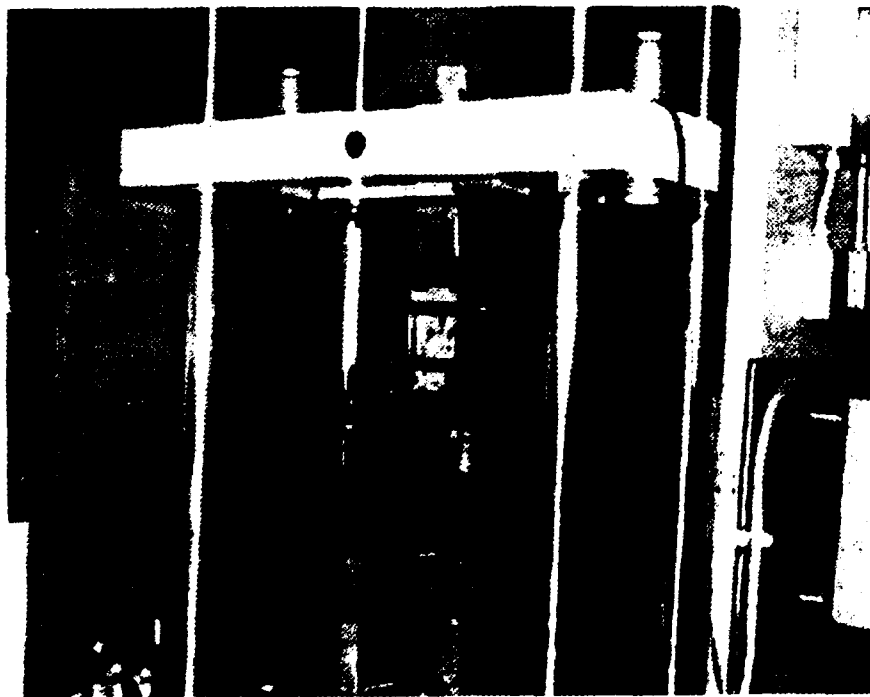


Fig. 3-3: The Modified Boeing Compression After Impact Fixture.

4. TEST RESULTS AND DISCUSSION

4.1. IMPACT RESULTS

Eight of the specimens received impacts ranging from 2.35 ft-lbs (3.19 J) to 11.7ft-lbs (15.4 J). Two impacts were done for each energy level.

As the impactor's energy is imparted to the specimen, the impactor slows down until all the kinetic energy is transferred to the specimen and the frame. This is usually at the point of the highest load. Some of this energy causes the impactor to rebound in the opposite direction. The difference between the impact and the rebound energy is the amount of energy absorbed by the specimen by damage and vibration. The energy levels reported herein are the maximum values which occur very close to the maximum load.

The impact fixture will also absorb some energy by vibration. However, since the fixture and support are so stiff and massive, this is negligible.

Impacts at 2.35 and 2.385 ft-lbs (3.19 & 3.23 J) only dented the specimens (Appendix figures A-1 to A-4). At this energy level, the "C"-scan detected a small amount of interior damage (Appendix figures A-17 and A-19). The force versus time curves, shown in Figures 4-1 and 4-2, were smooth and symmetrical. Energy versus time curves show a maximum energy at the maximum force. A final energy as the force curves returned to zero show 30 percent of the energy was imparted to the specimens and fixture. The first data points of the impact were missed by the oscilloscope because the trigger level was set too high. This mistake caused the force versus displacement curves to be inaccurate.

SPECIMEN #A3

2.35 FT-LBS, MASS = 17.87 LBS

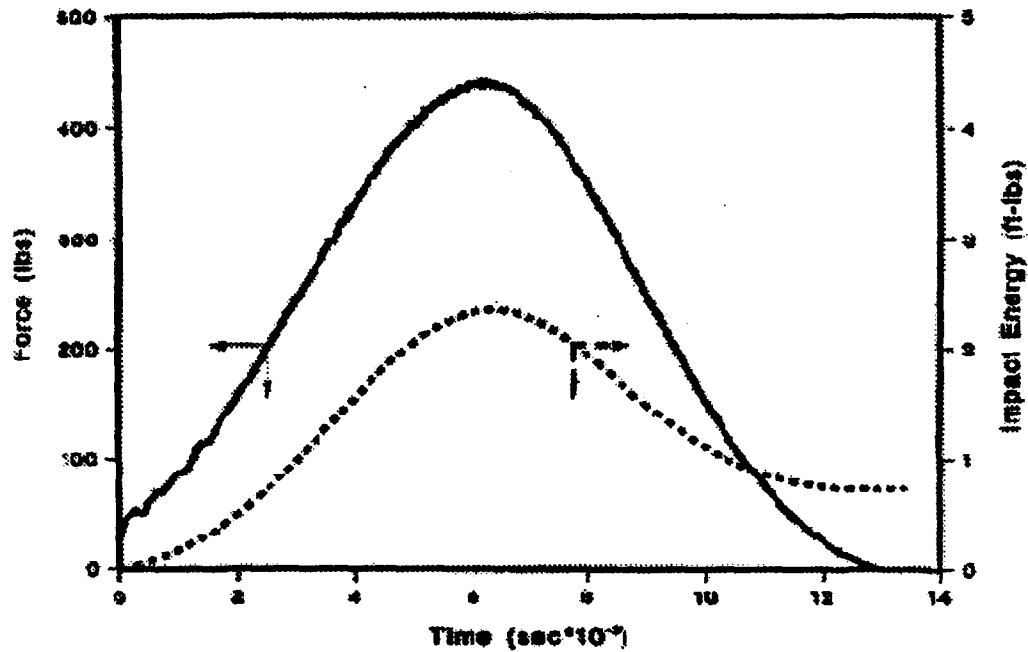


Fig. 4-1: Force and Energy vs. Time Plot for Specimen A3.

SPECIMEN #A4

2.385 FT-LBS, MASS = 17.87 LBS

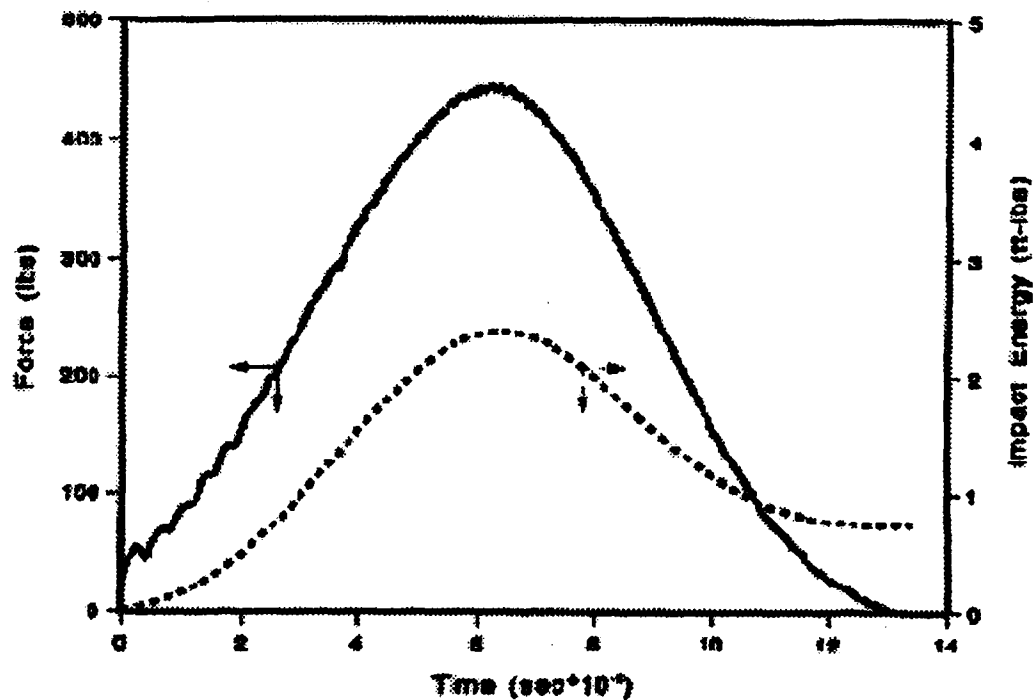


Fig. 4-2: Force and Energy vs. Time Plots for Specimen A4.

At 5.45 ft-lbs (7.44 J) and 5.54 ft-lbs (7.51 J), back face cracks appeared (Appendix figures A-5 to A-8). The cracks were oriented 90 degrees to the aramid fiber direction. This crack orientation can be explained by the stretching of the material during processing. Interior damage stayed within the boundaries of the dent.

The force versus time curves show jagged or sudden drops in impact load just before the maximum impact load. These drops or vibrations damped out before the maximum impact load. Again, the maximum impact force coincided with the maximum impact energy. At the end of the impact event, a final energy absorbed by the specimens and/or impact fixture was around 55 percent (Figures 4-3 and 4-4).

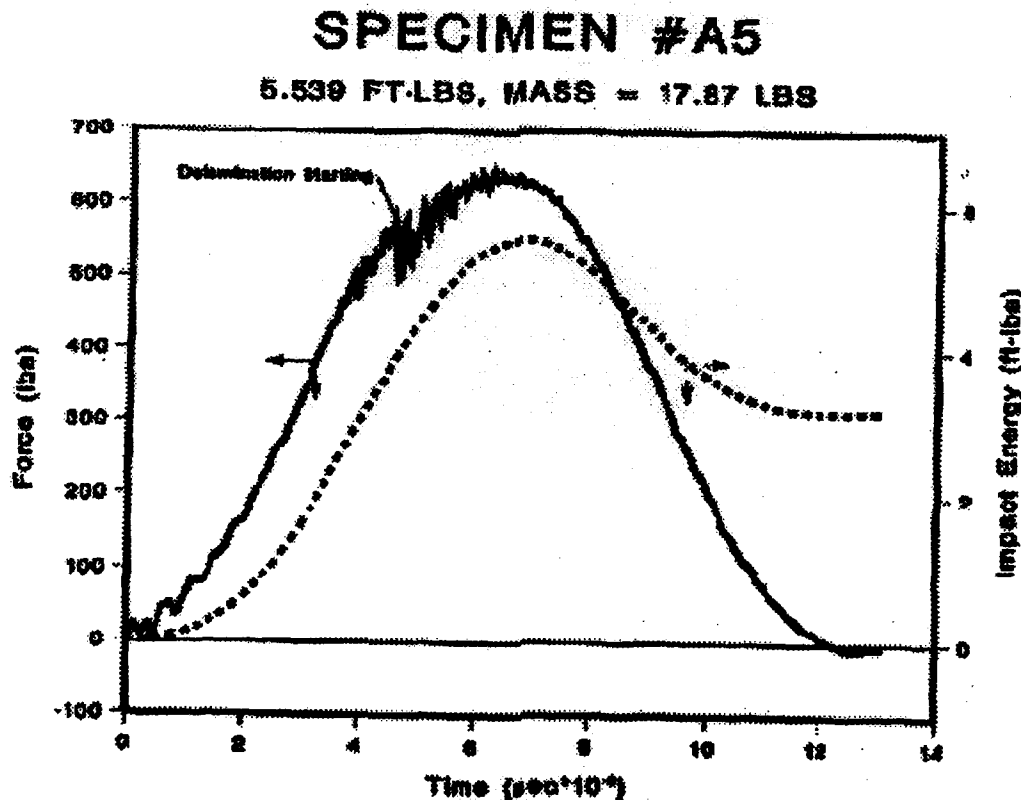


Fig. 4-3: Force and Energy vs. Time for Specimen A5

SPECIMEN #A6

5.498 FT-LBS, MASS = 17.87 LBS

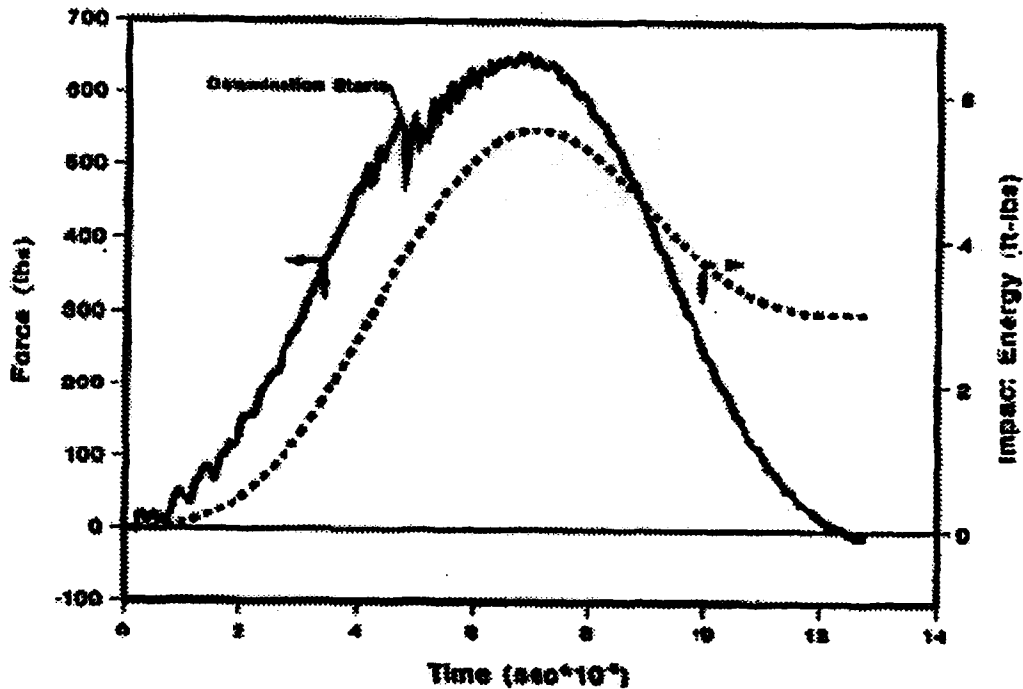


Fig. 4-4: Force and Energy vs. Time for Specimen A6

Force versus displacement curves also show the damage behavior previously described (Figures 4-5 and 4-6). Johnson (Ref. 2) related similar jags or sudden drops in load to delamination of the aramid/adhesive layers from the aluminum layers in static indentation load tests.

There is no quantitative way of relating the drops in load to delamination in the impact testing. The impact event happens too fast to relate the drops or vibrations in impact load to damage of the panel because of impact.

Unfortunately, the initial data from the less damaged specimens wasn't picked up by the Nicolet, so no comparison can be made between the two energy levels.

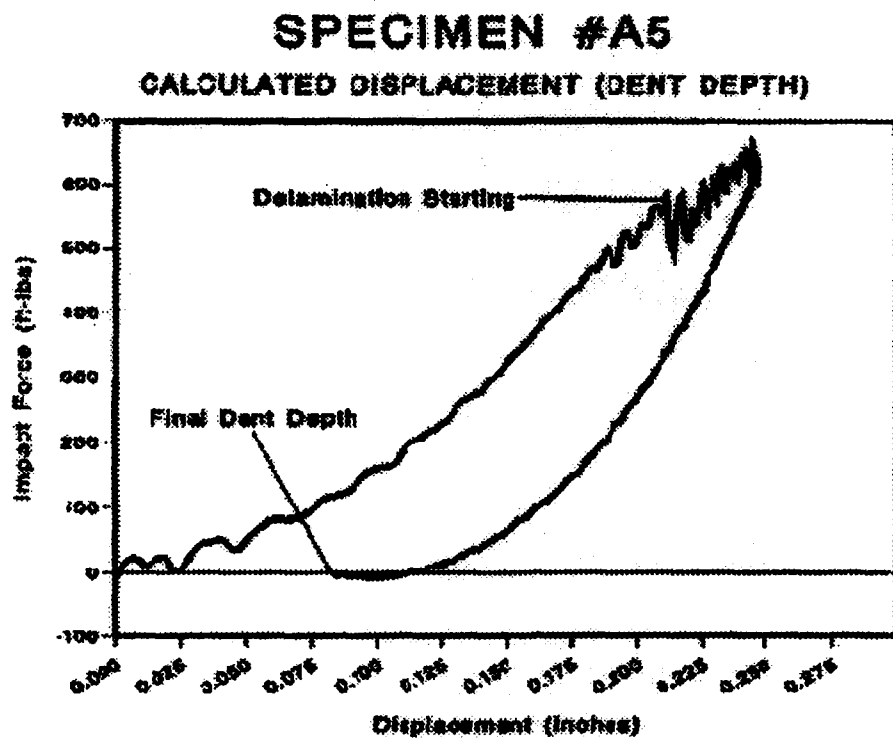


Fig. 4-5: Force vs. Calculated Displacement for Specimen A5

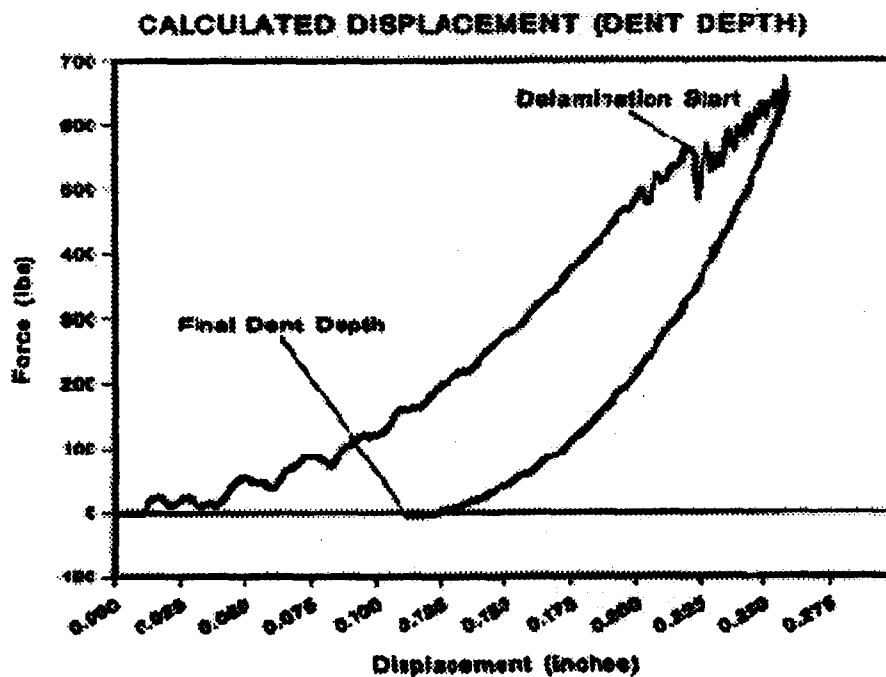


Fig. 4-6: Force vs. Calculated Displacement for Specimen A6.

The ARALL®-1 laminates impacted at above 10 ft-lbs (13 J) were penetrated. Penetration is defined as the imbedding of the impactor nose or "tip" in the impact specimen so that the impactor cannot rebound back through the timing gate. At 10.31 ft-lbs (14.00 J), the ARALL®-1 laminate was totally penetrated. Specimens A-7 through A-10 received impacts at 10.31 ft-lbs (14.00 J), 10.45 ft-lbs (14.20 J), 11.69 ft-lbs (15.8 J), and 11.7 ft-lbs (15.9 J). All four specimens were penetrated at these impact energy levels (Appendix figures A-9 and A-16).

At these impact energy levels, force versus time curves show gradual increase in load until a sudden drop. This drop indicates an interior failure such as a crack or delamination. Though the load may increase, the surrounding material will continue to carry the load until the crack grows or the failure of the surrounding material occurs. The energy versus time curves always increase with the maximum impact force occurring at the same time as the slope of the energy versus time curve starts to decrease. The final energy absorbed by the specimen is 100 percent.

As the specimen is penetrated, the impact load drops off. This is shown by a steep drop in the impact force curve and a corresponding sudden slope change in the impact energy curve that was not shown in the lower impact energies (Figures 4-7 to 4-10).

SPECIMEN #A7

10.45 FT-LBS, MASS = 17.87 LBS

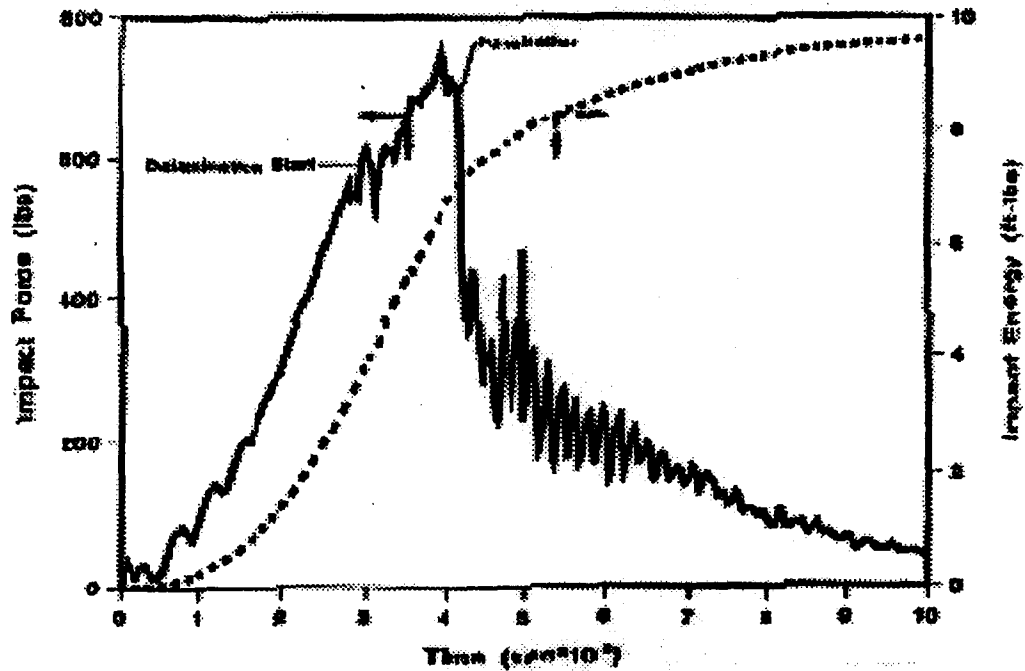


Fig. 4-7: Force and Energy vs. Time for Specimen A7.

SPECIMEN #A8

10.31 FT-LBS, MASS = 17.87 LBS

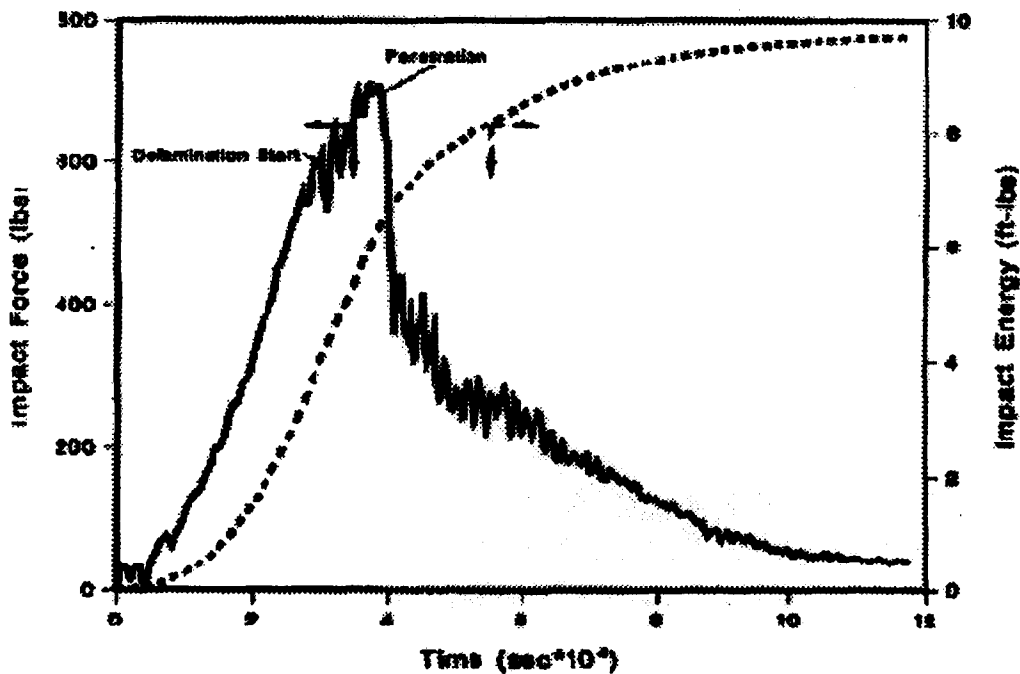


Fig. 4-8: Force and Energy vs. Time for Specimen A8.

SPECIMEN #A9

11.7 FT-LBS, MASS = 17.87 LBS

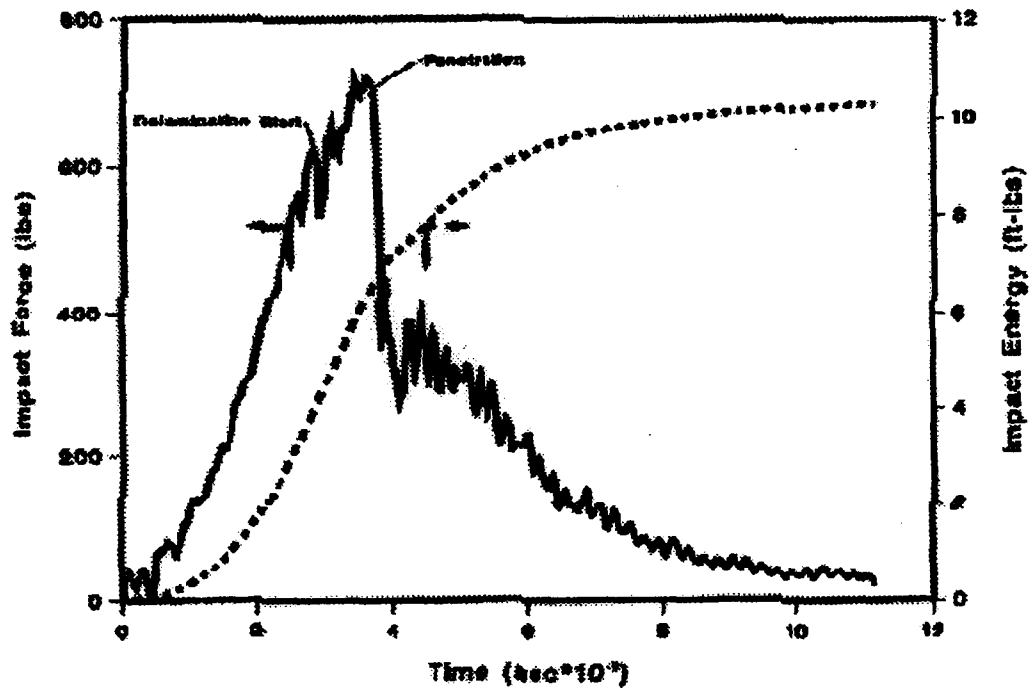


Fig. 4-9: Force and Energy vs. Time for Specimen A9.

SPECIMEN #A10

11.69 FT-LBS, MASS = 17.87 LBS

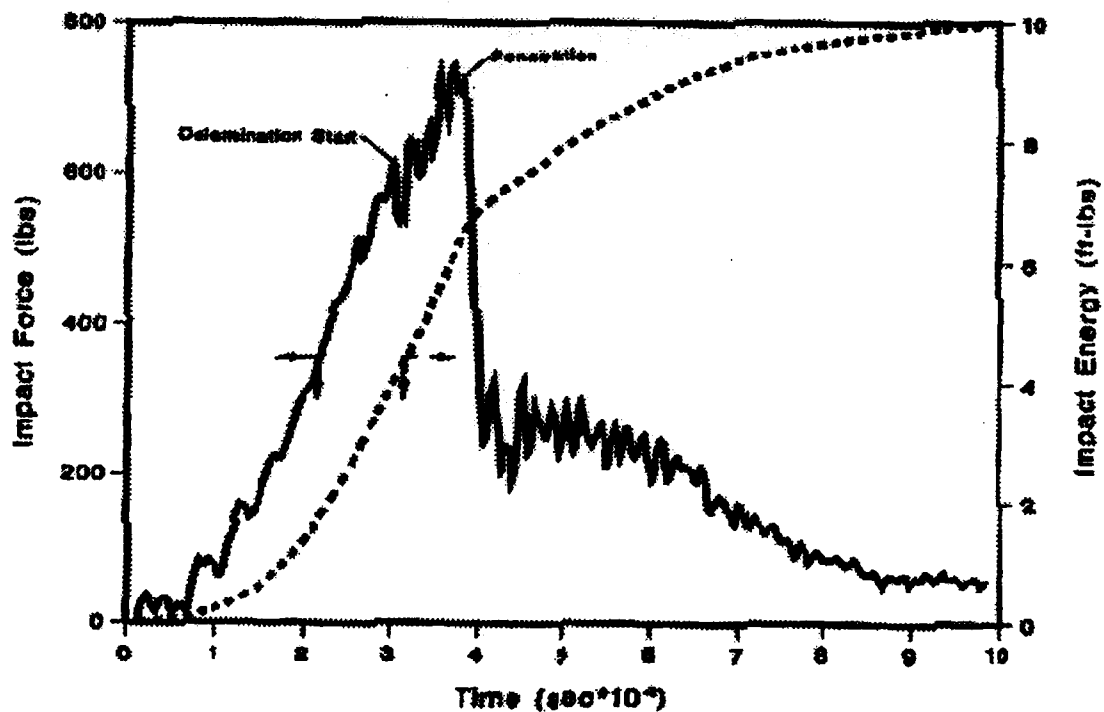


Fig. 4-10: Force and Energy vs. Time for Specimen A10.

On comparison with Graphite/Epoxy composites, the ARALL[®]-1 laminates lose less load during the cracking. The aluminum seems to be acting as an energy absorber, plastically absorbing energy.

Figure 4-11 shows the energy lost to the specimen and fixture through vibration or damage versus impact energy. Several other materials are shown for comparison such as graphite/epoxy (Ref. 5) and fiberglass sheet molding compound, a random oriented fiberglass impregnated polyester resin (Ref. 6). According to these data, Arall[®]-1 laminates require less impact energy than the graphite/epoxy or the SMC to cause the same energy absorption. However, if the impact energy is normalized by the specimen thickness, as in Figure 4-12, ARALL[®]-1 laminates require more energy per specimen thickness for the same amount of energy absorption.

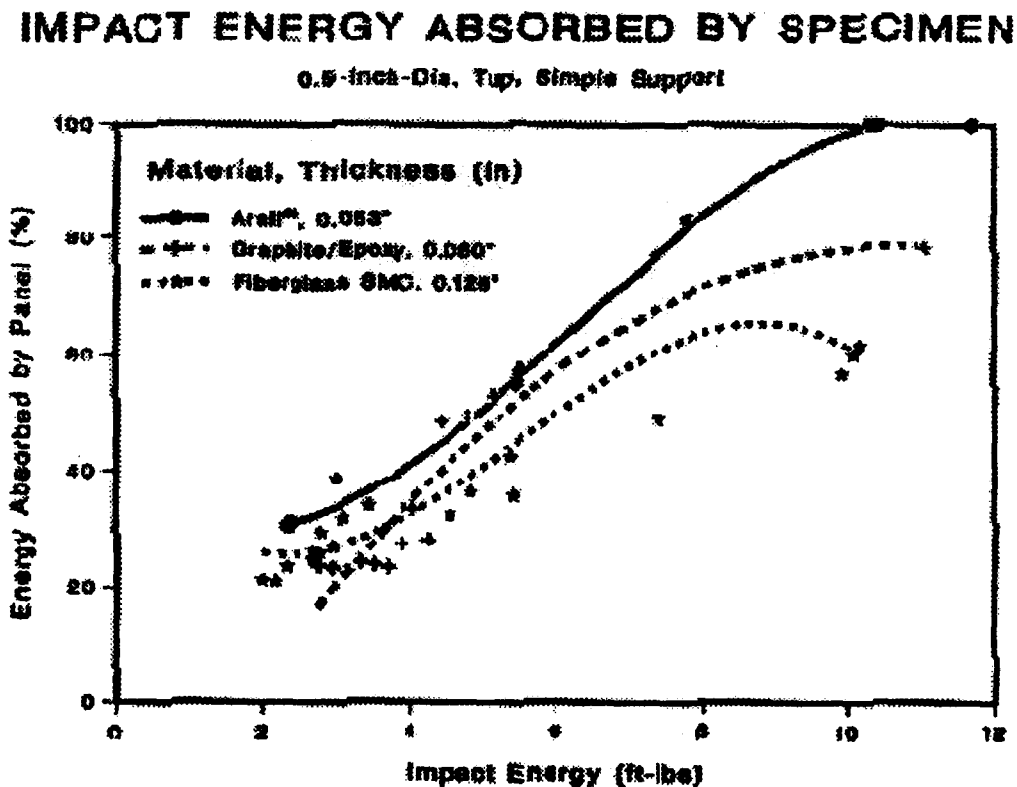


Fig. 4-11: Energy Absorbed vs. Impact Energy.

IMPACT ENERGY ABSORBED BY ARALL SPECIMEN

0.5-Inch-Dia. Tip, 150mm I.D. Simple Support

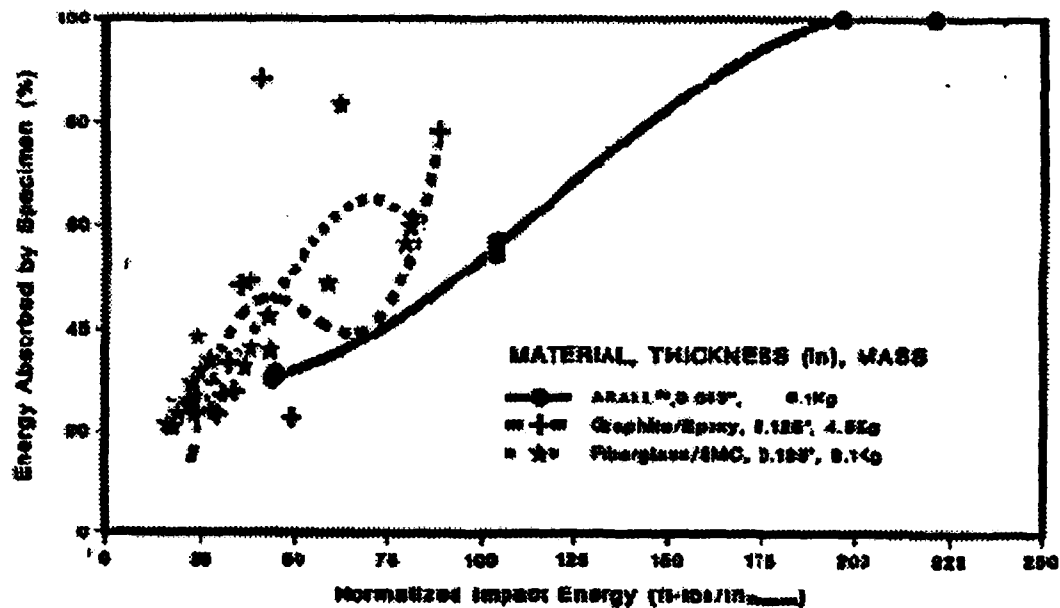


Fig. 4-12: Energy Absorbed vs. Normalized Impact Energy.

Figure 4-13 plots normalized impact damage area as measured by "C" scan damage area versus normalized impact energy for ARALL[®]-1 (odd-numbered Appendix figures A-17 thru A-31), graphite/epoxy, and fiberglass SMC. ARALL[®]-1 requires more energy to cause equivalent damage compared to the other two materials for normalized impact energies greater than 100 ft-lbs/in.

ARALL[®] NORMALIZED IMPACT ENERGY vs. NORMALIZED "C" SCAN DAMAGE

0.5" Dia. Tup. 100mm I.D. Ring, Simple Support

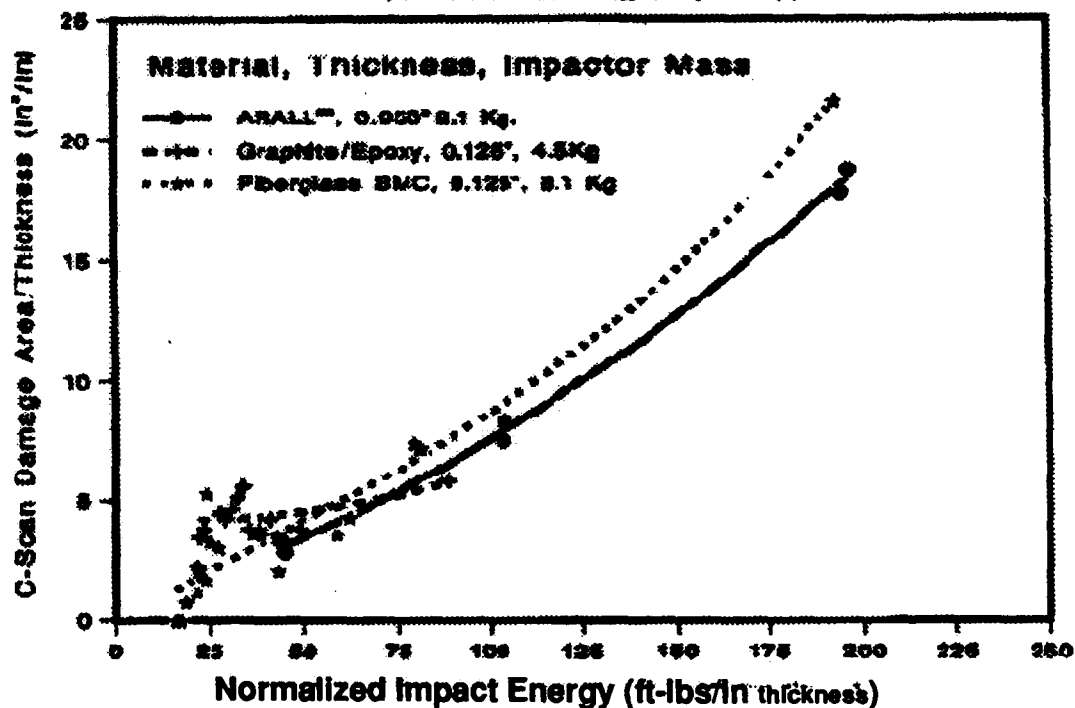


Fig. 4-13: Normalized Damage Area vs. Normalized Impact Energy.

However, the ARALL[®]-1 laminates are penetrated at 10 ft-lbs (13.56 J), shown in Appendix figures A-9 thru A-16, as compared with over 40 ft-lbs (54.2 J) for graphite/epoxy and 25 ft-lbs (33.9 J) for fiberglass SMC.

Table 4-1 summarizes the impact test results. In this table, E_{ki} is the impact energy, and E_{loss} is the percent energy absorbed by the specimen.

TABLE 4-1

Specimen #	Tup Diameter (in.)	Mass (lbs)	Vin (ft/s)	E _{ki} (ft-lbs)	E _{loss} (%)	Impact Force (lbs)	Damage Area (in ²)
A3	0.5	17.87	2.91	2.35	30.6	440	0.173
A4	0.5	17.87	2.93	2.39	31.3	445	0.15
A5	0.5	17.87	4.47	5.54	57	560	0.442
A6	0.5	17.87	4.45	5.49	54.9	540	0.399
A7	0.5	17.87	6.14	10.45	100	590	0.994
A8	0.5	17.87	6.1	10.31	100	600	0.939
A9	0.5	17.87	6.5	11.69	100	600	1.227
A10	0.5	17.87	6.49	11.7	100	610	0.932

ARALL[®]-1 IMPACT RESULTS

4.2. COMPRESSION RESULTS

The compression loading of the specimens showed there was no real dropoff in compression strength after the impact. Unfortunately, the specimens were so thin, even the undamaged samples buckled around 5000 psi (34.4 MPa), and many of the impacted specimens started to buckle upon application of load. This is shown by the stress-strain diagrams, Figures 4-14 through 4-23. They failed similarly to aluminum and steel specimens in that the buckling occurred in the top half of the specimen (Ref. 5).

An initial modulus calculated from the average of the six gauges on the undamaged panels showed an average initial compression modulus of 11.2 MSI. This value is taken from just before the onset of buckling while all the back-to-back strain gauge pairs were tracking each other. Goodyear and Chellman reported a modulus of 10.7 MSI for ARALL®-1 in the L direction (Ref. 7).

Table 4-2 is a tabulation of the strain gauge readings, the compressive stress, and the calculated initial moduli for A1 & A2.

Table 4-2

Specimen	Stress (PSI)	Modulus @Gauge # (MSI)						AVE (MSI)
		# 1	# 2	# 3	# 4	# 5	# 6	
A1	-4064.15	12.1	11.8	16	8.76	9.03	7.49	10.8
A2	-4116.98	11.8	14.2	10.6	11	9.64	12.5	11.6

INITIAL MODULI FOR UNDAMAGED SPECIMENS

Manieri reported a Young's Modulus of 8.9 Msi for undamaged graphite/epoxy composites using the same modified compression after impact fixture (Ref. 5). This compared well with numerical analysis which gave a Young's Modulus of 9.31 Msi. Standard composite compression tests, ASTM D695 and ASTM D3410, gave average Young's Moduli of 7.7 Msi and 7.3 Msi, respectively.

ARALL SPECIMEN #A1

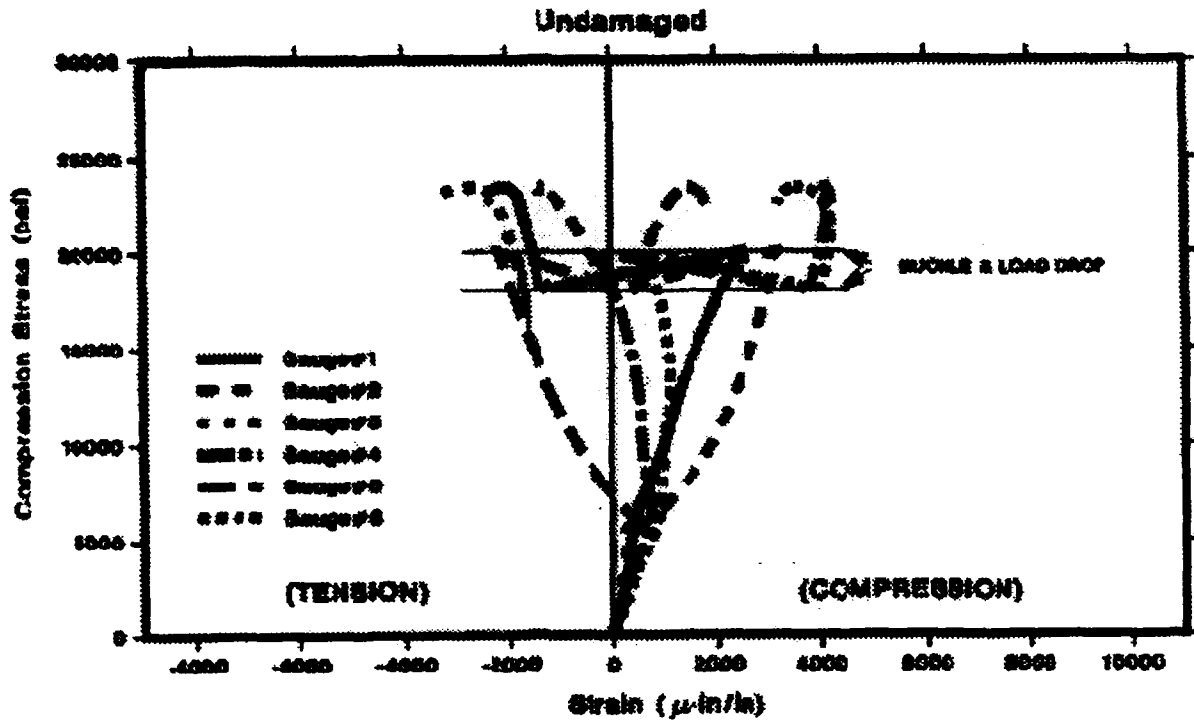


Fig. 4-14: Stress-Strain Curves for Specimen A1.

ARALL SPECIMEN #A2

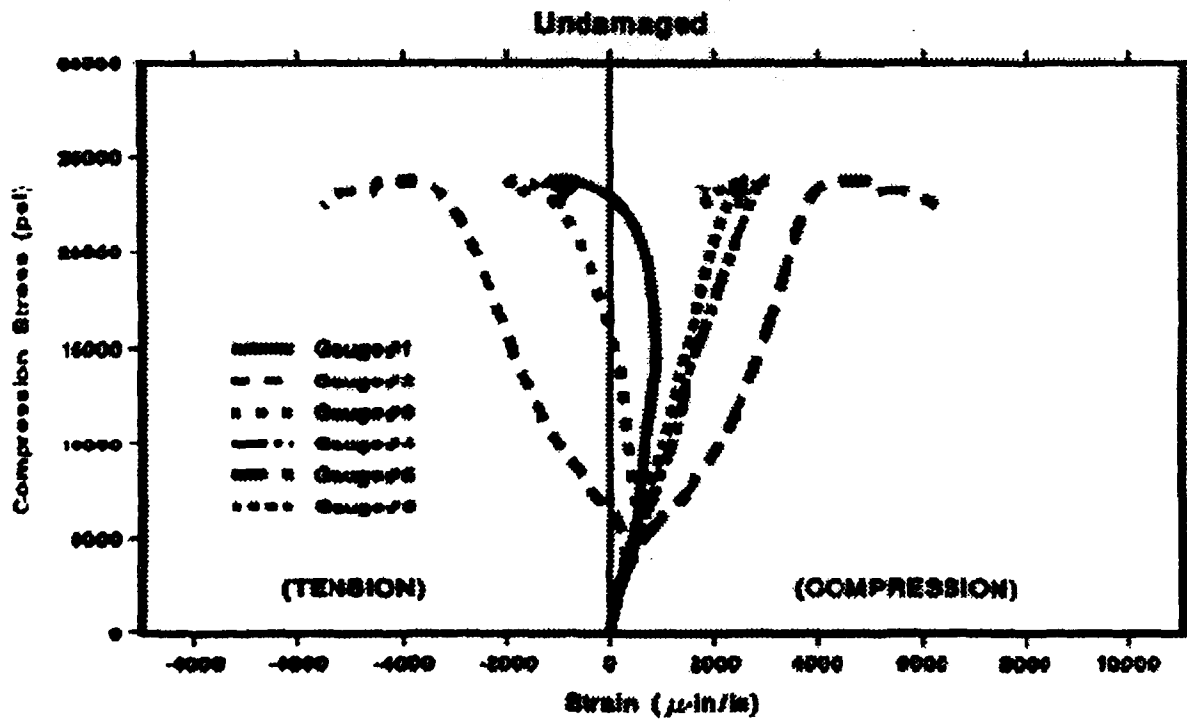


Fig. 4-15: Stress-Strain Curves for Specimen A2.

ARALL SPECIMEN #A3

2.35 ft-lb Impact

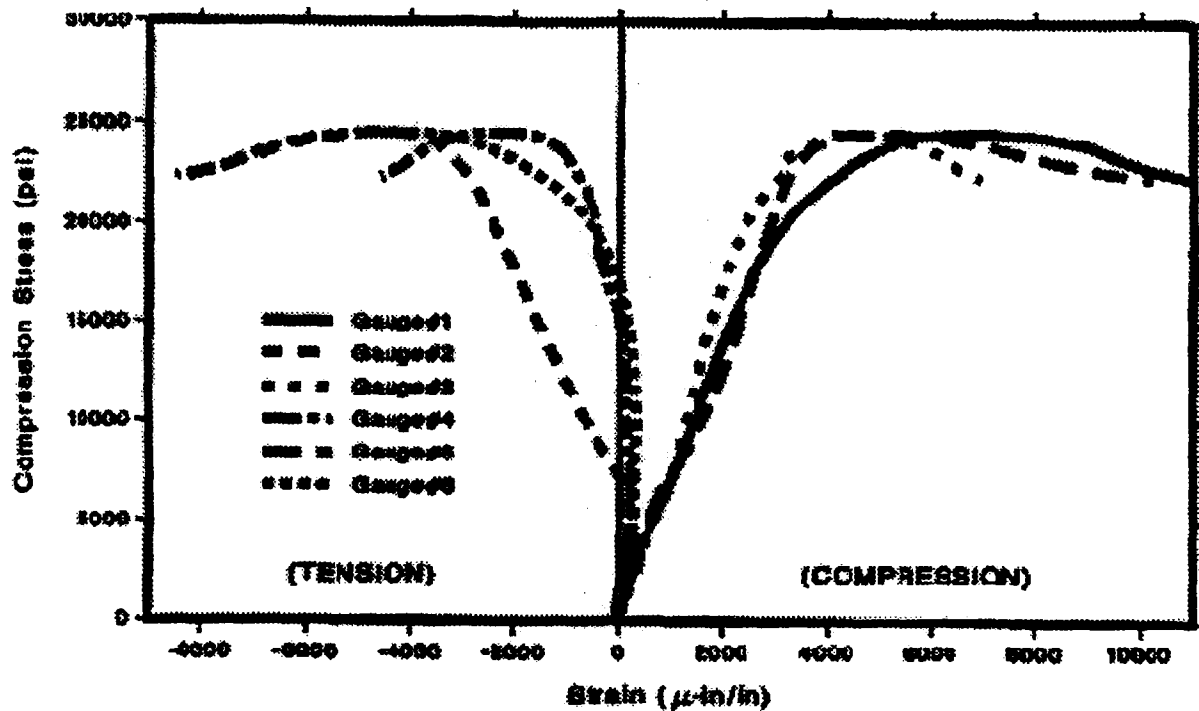


Fig. 4-16: Stress-Strain Curves for Specimen A3.

ARALL SPECIMEN #A4

2.39 ft-lb Impact

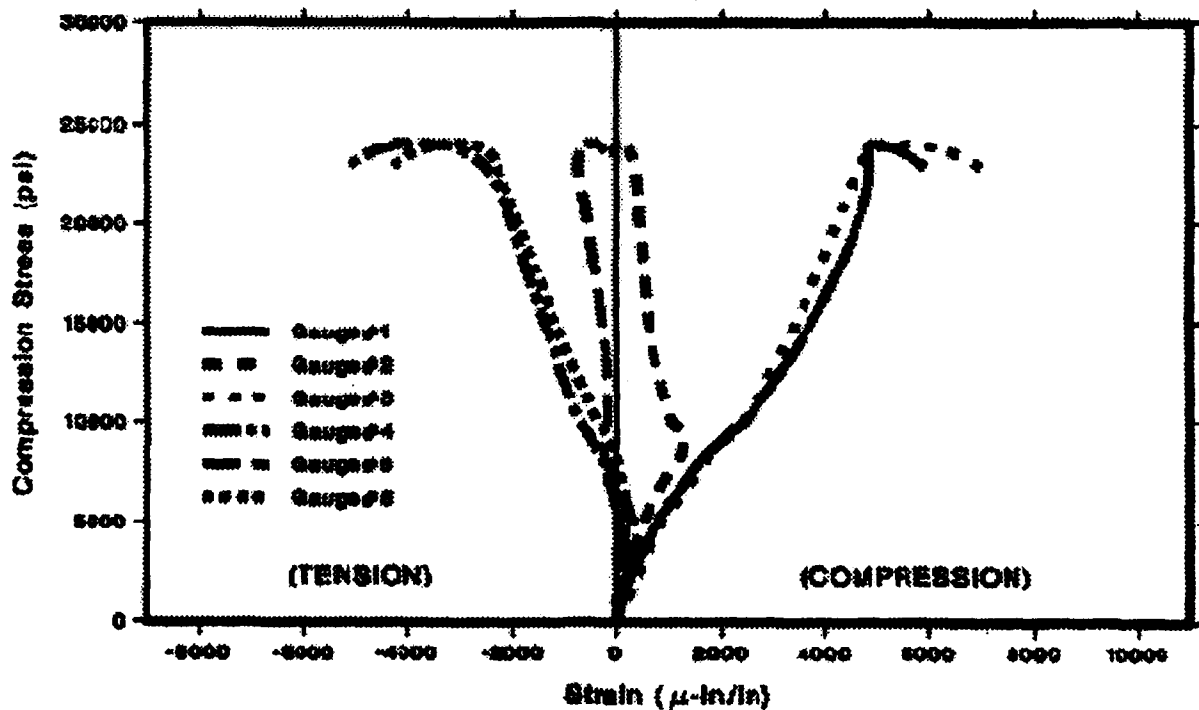


Fig. 4-17: Stress-Strain Curves for Specimen A4.

ARALL SPECIMEN #A5

5.539 ft-lbs Impact

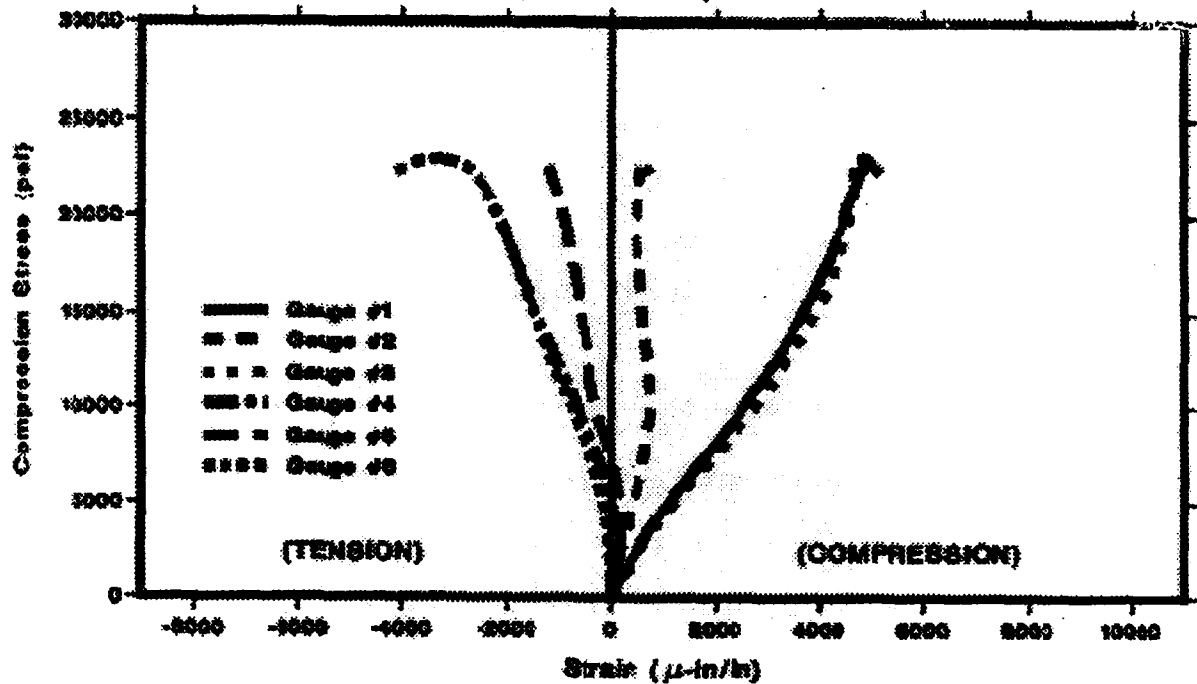


Fig. 4-18: Stress-Strain Curves for Specimen A5.

ARALL SPECIMEN #A6

5.48 ft-lb Impact

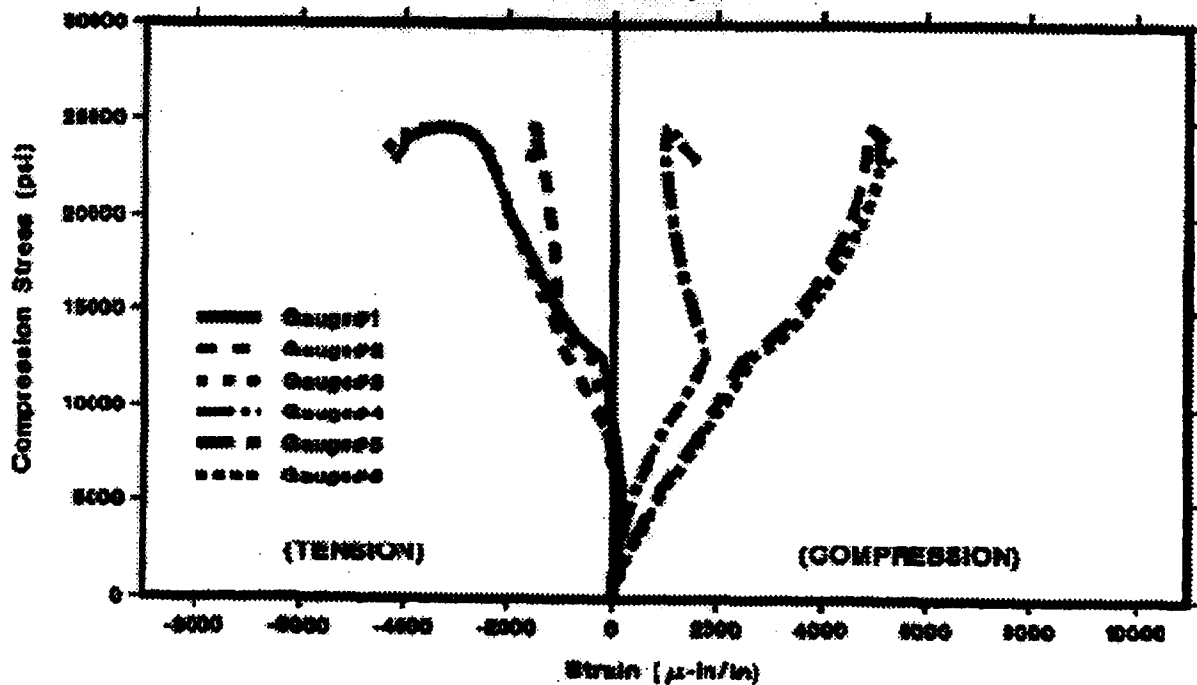


Fig. 4-19: Stress-Strain Curves for Specimen A6.

ARALL SPECIMEN #A7

10.45 ft-lb Impact

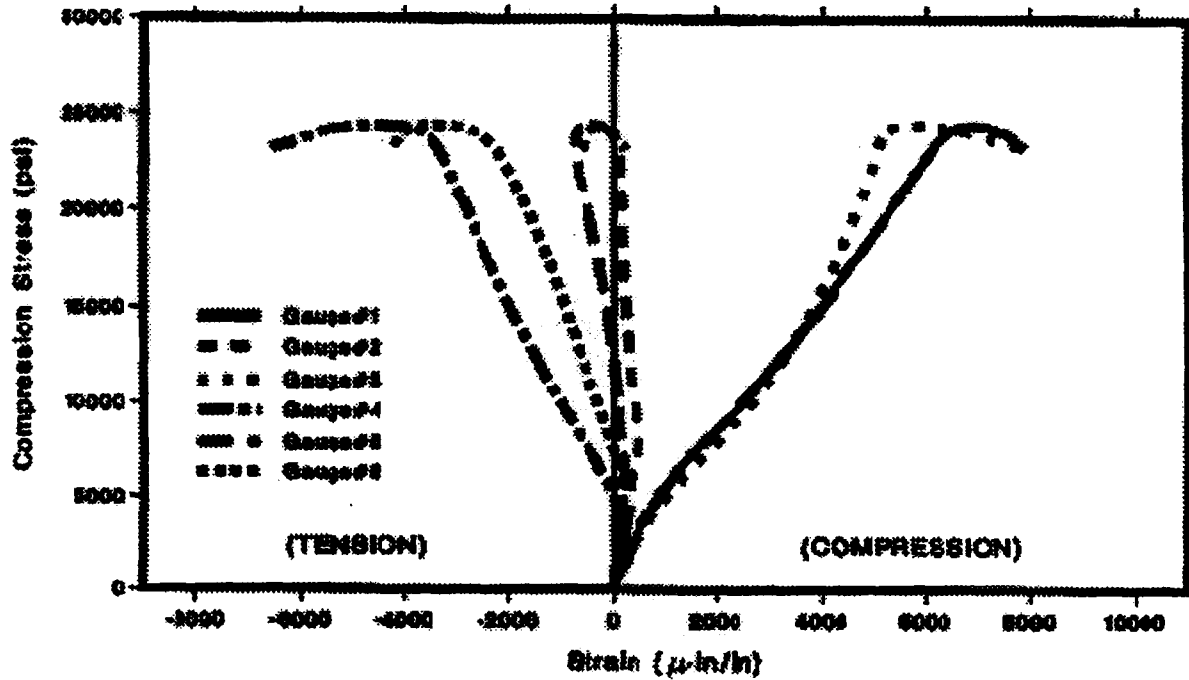


Fig. 4-20: Stress-Strain Curves for Specimen A7.

ARALL SPECIMEN #A8

10.31 ft-lb Impact

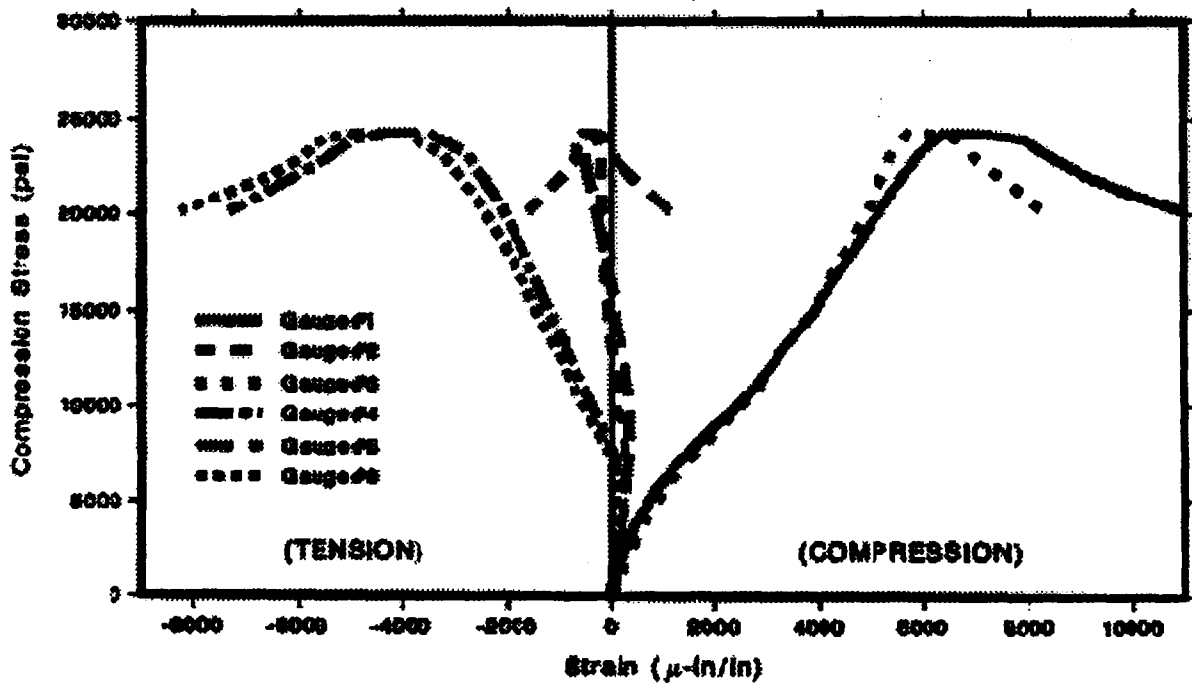


Fig. 4-21: Stress-Strain Curves for Specimen A8

ARALL SPECIMEN #A9

11.7 ft-lb Impact

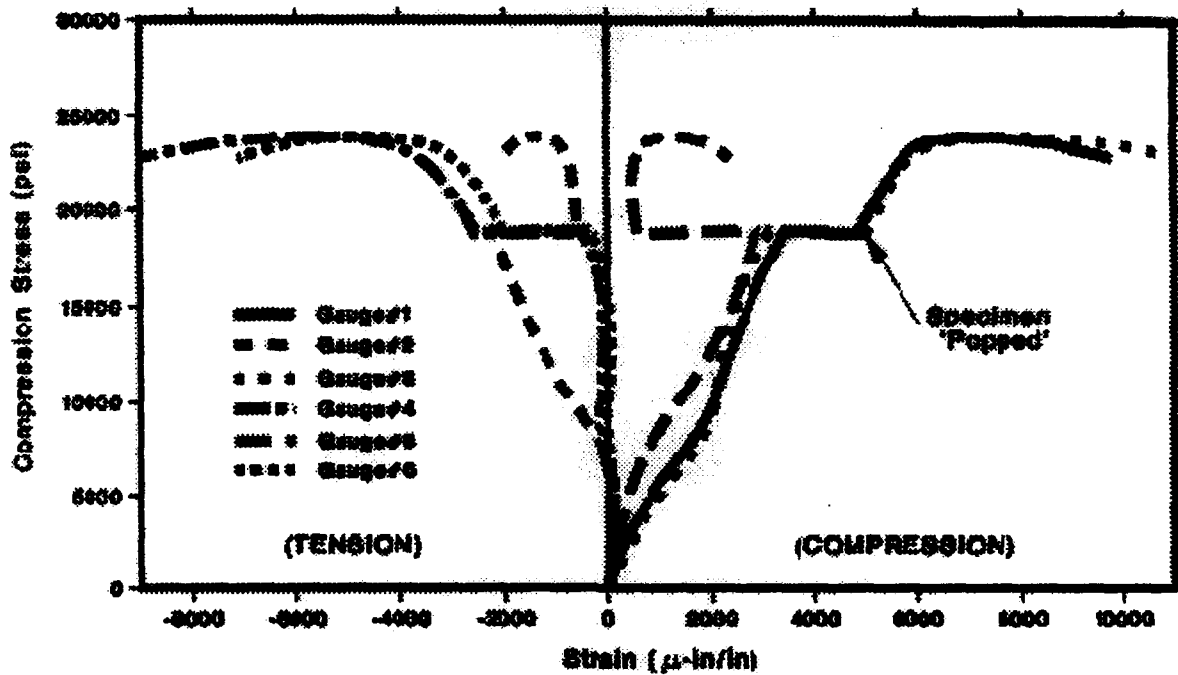


Fig. 4-22: Stress-Strain Curves for Specimen A9.

ARALL SPECIMEN #A10

11.69 ft-lb Impact

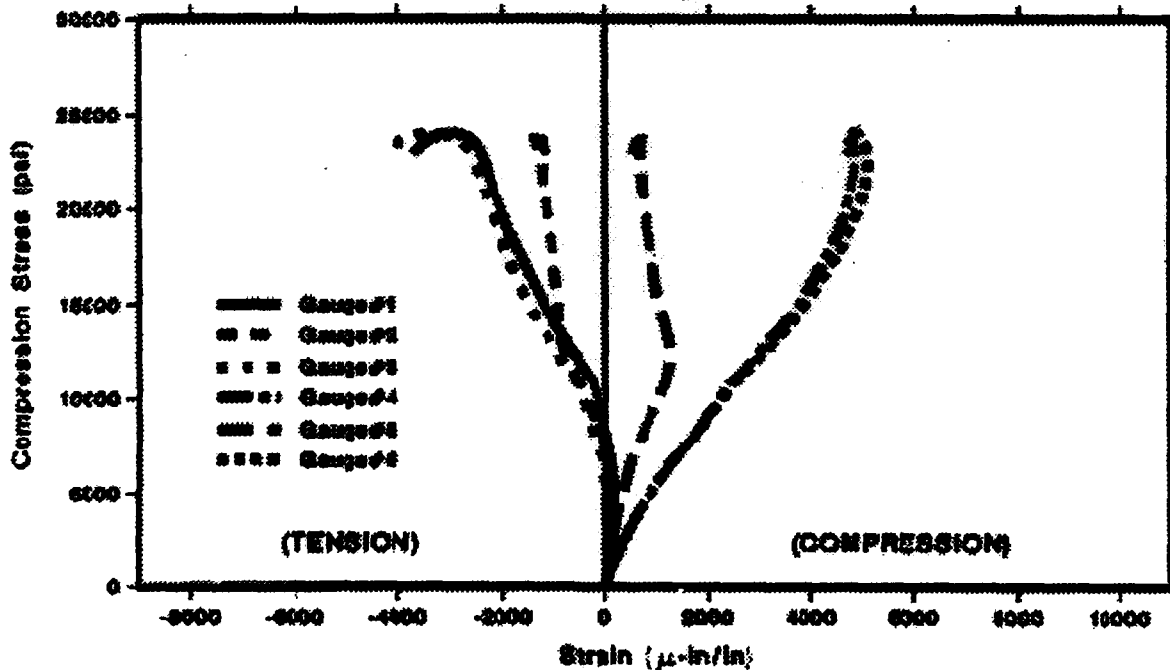


Fig. 4-23: Stress-Strain Curves for Specimen A10.

In a good compression failure, the back-to-back strain gauges track each other. They diverge when the impact induced damage starts to grow or buckling commences.

If the back-to-back strain gauges do not track each other, the specimen has unequal loading. Additionally, thin specimens have a much lower buckling load. This lower load allows global buckling of the specimen before the damaged regions have a chance to initiate specimen failure. Manieri and Harmsworth documented this effect in Graphite/Epoxy composites (Ref. 5).

The compression after impact fixture is designed to "force" the failure to initiate in the damaged section of the specimen. If the damaged section does not initiate the failure, the specimen will fail at a point of stress concentration such as the constrained ends or in a noncompression mode such as buckling.

The undamaged specimens started buckling at around 5500 psi. The specimens damaged at 2.4 ft-lbs started buckling at around 3000 psi. Above 5 ft-lbs, the panels started buckling almost with the initial application of load. In all of the tests, the gauges to the sides of the impact areas and on the same side (#1 & #3 or #4 & #6) tracked each other well after buckling initiation. This indicates the lack of true compression in our specimen in this compression fixture. The most likely explanation seems to be the thickness of the specimens. The wide divergence in stress-strain readings made calculating an average modulus for the impacted specimens guesswork.

All the specimens were loaded up until they started to deform and would not carry any more load. Two specimens redistributed the load (Figures 4-14 and 4-22). These effects are considered to be fixture dependent since they happened in both the damaged and the undamaged specimens.

ARALL[®] IMPACT ENERGY vs. CAI STRENGTH

0.5 Inch Dia. Tip, Simple Support, 100mm Ring

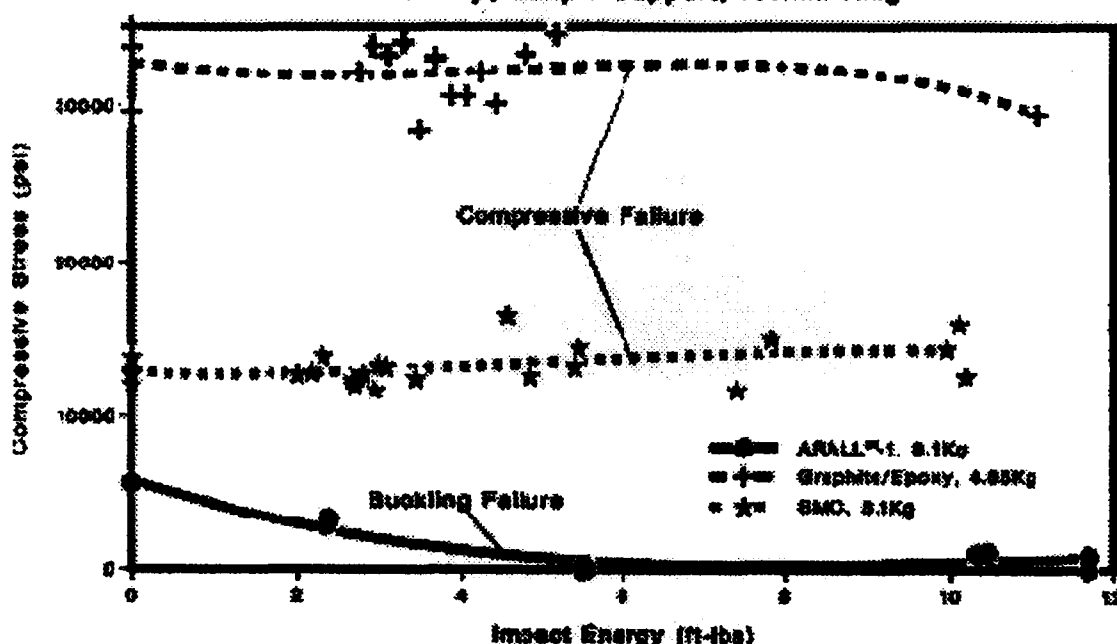


Fig. 4-24: Compression After Impact Strength vs. Impact Energy.

Figure 4-24 illustrates buckling initiation load with increasing impact energy. Also graphed are the compression-after-impact (CAI) strengths of graphite/epoxy and fiberglass SMC for comparison.

Comparing the Compression After Impact Behavior of ARALL[®] laminates with that of graphite epoxy composites, and fiberglass SMC composites is difficult because of the different failure mechanisms. The ARALL[®]-1 laminates fail by global buckling followed by yielding of the specimen. SMC and graphite epoxy fail due to local buckling of the damaged area of the specimen which initiates unstable delamination growth. This type of failure occurs at higher compressive loads than global buckling.

Table 4-3 shows the Compression After Impact data for ARALL[®]-1 laminates. Specimens A5, A6, and A9 buckled almost immediately upon application of compression load.

Table 4-3

Specimen #	Impact Energy (ft-lbs)	Buckling Load (lbs)	Buckling Stress (psi)	Initial Modulus (msi)
A1	0	-1473	-5558	10.9
A2	0	-1482	-5592	11.6
A3	2.35	-733	-2776	15.3
A4	2.39	-850	-3207	13.2
A5	5.54	0	0	18.3
A6	5.49	0	0	12.4
A7	10.45	-286	-1079	17
A8	10.31	-256	-966	1.66
A9	11.69	0	0	2.51
A10	11.7	-227	-856	2.02

COMPRESSION AFTER IMPACT RESULTS

ARALL®-1 laminates lose about half their compressive buckling load owing to impact energies of about 2 ft-lbs. At impact energies of 5ft-lbs and greater, the ARALL®-1 laminates start buckling almost immediately.

"C"-scans taken of the specimens after testing show no growth of any of the damaged areas. This indicates the damaged area was not the initiation point of these specimen failures. Compression buckling failure occurred because of the thinness of the samples.

5. CONCLUSIONS

During low velocity impact, ARALL®-1 laminates dent like metals as opposed to delaminating like composites. This is indicative of plastic deformation.

During impact, ARALL®-1 laminates don't vibrate as much as layered composites. Sheet Molding Compound, which has randomly oriented reinforcement, also exhibits this behavior. This may be based on "isotropic" properties or specimen geometry effects.

Above 2.5 ft-lbs, ARALL®-1 laminates show cracks on the back face side of the laminate. The cracks run perpendicular to the fiber direction. This may due to residual stresses caused by the stretching operation.

Specimens A5 and A6 show an increase of vibration before a maximum impact force. This indicates damage and delamination growth. In composites, this dropoff is sudden and larger. The increasing vibration is either matrix cracking or separation of the adhesive from the aluminum.

As the "C"scans show, any impact damage is restricted to the immediate dent area or within 1/4 inch of the penetration. Comparable damage would be much greater in an organic matrix composite.

A threshold of penetration for this thickness of ARALL®-1 appears to be between 5 and 10 ft-lbs. Fibers aren't broken through until at least 10 ft-lbs.

Compressive buckling was achieved in the modified Boeing Compression fixture for the thickness of the ARALL®-1 material. The buckling load for the specimens was reduced by increasing impact energy levels.

6. RECOMMENDATIONS

A thicker ARALL®-1 laminate should be used for any more follow-on work. This will increase the likelihood of getting compression failures in the modified Boeing Compression fixture.

Thin ARALL®-1 laminates handle low velocity impacts by denting, a metal like behavior. This makes them good candidates for impact areas like lower aircraft skins.

7. REFERENCES

1. NASA RP 1142, **NASA/Aircraft Industry Standard Specification for Graphite Fiber/Toughened Thermoset Resin Composite Material**, June 1985
2. W.S. Johnson, **Impact and Residual Fatigue Behavior of ARALL and AS/5245 Composite Materials**, NASA Technical Memorandum 89013, October 1986
3. P. Sjöblom, SAMPE International Symposium, 32, 529, 1987
4. Sjöblom, Hartness, and Cordell, **On Low Velocity Impact Testing of Composite Materials**, Journal of Composites, Jan 1988.
5. Manieri and Harmsworth, **Compressive Properties of Damaged Graphite/Epoxy Composites**, AFWAL-TM-86-102, Nov., 1986
6. Hoogsteden, **Post-Impact Compression of SMC Fiberglass**, MS87-557, Presented at Fabricating Composites '87, Sept., 1987
7. Goodyear and Chellman, **Material Characterization of ARALL®-1 and 2 Laminates.**, Lockheed-Georgia GA-21787.4, Presented at the 1st ARALL® Conference, Oct, 1987

A.1. Specimen Photographs

Appendix



Fig. A-1: Impact Side of Specimen A3, 2.35 ft-lbs (3.19 J).



Fig. A-2: Backface Side of Specimen A3, 2.35 ft-lbs (3.19 J).

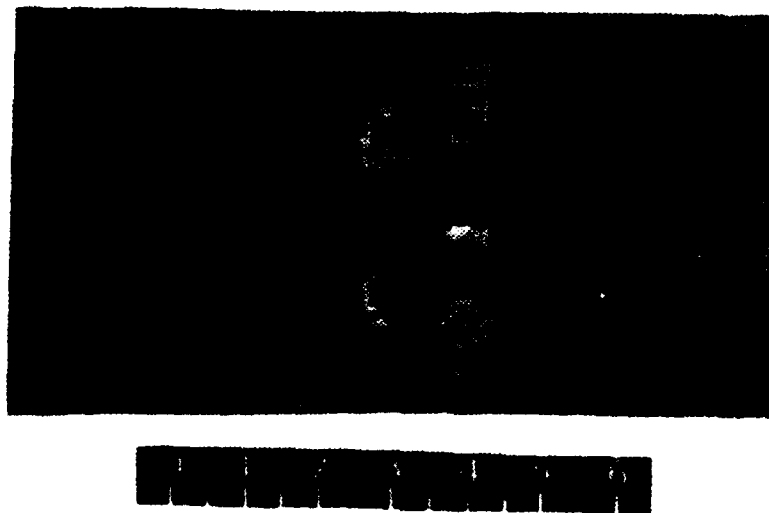


Fig. A-3: Impact side of Specimen A4, 2.29 ft-lbs (3.23 J).

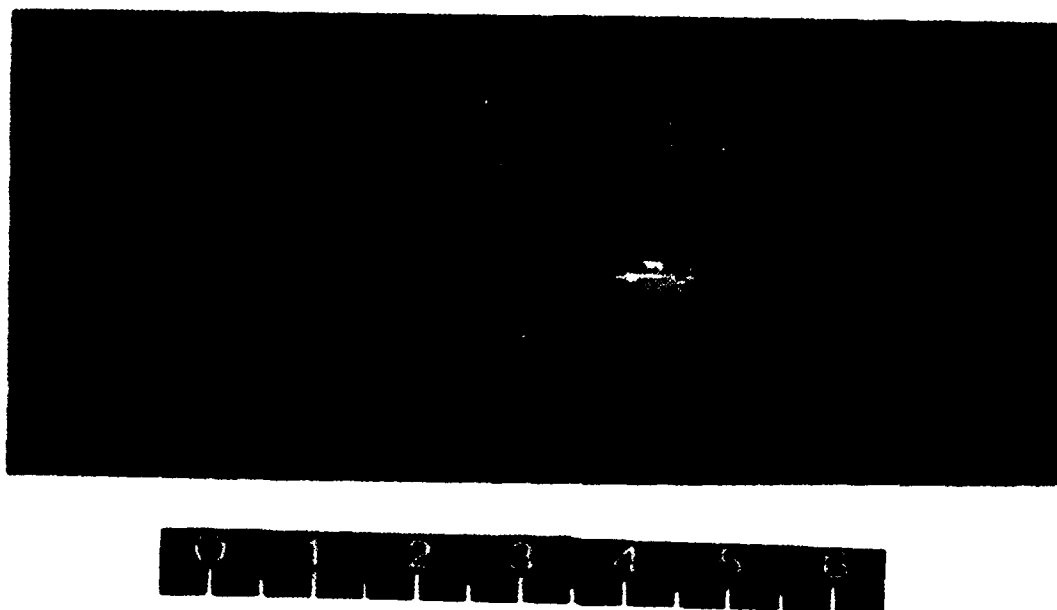


Fig. A-4: Back Side of Specimen A4, 2.29 ft-lbs (3.23 J).

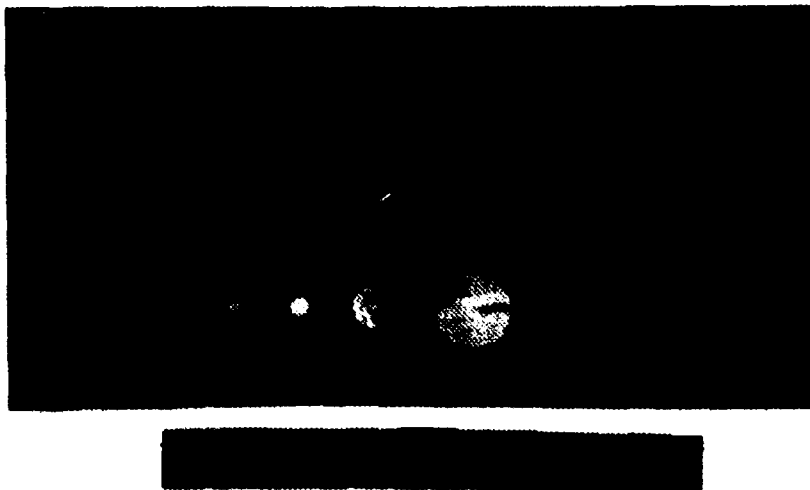


Fig. A-5: Impact Side of Specimen A5, 5.54 ft-lbs (7.51 J).



Fig. A-6: Back side of Specimen A5, 5.54 ft-lbs (7.51 J).



Fig. A-7: Impact Side of Specimen A6, 5.49 ft-lbs (7.44J).



Fig. A-8: Backside of Specimen A6, 5.49 ft-lbs (7.44 J).



Fig. A-9: Impact Side of Specimen A7, 10.45 ft-lbs (14.2J).



Fig. A-10: Back Side of Specimen A7, 10.45 ft-lbs (14.2 J).



Fig. A-11: Impact side of Specimen A8, 10.31 ft-lbs (14 J).

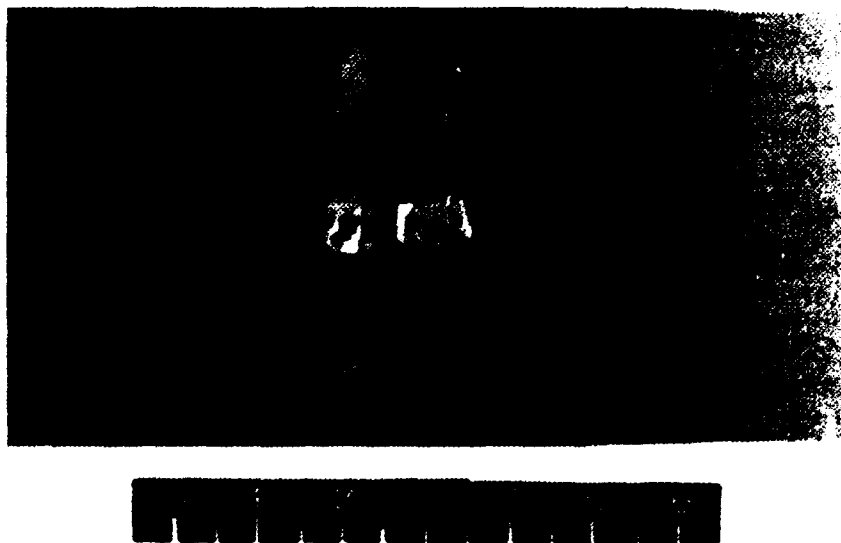


Fig. A-12: Back Side of Specimen A8, 10.31 ft-lbs (14 J).

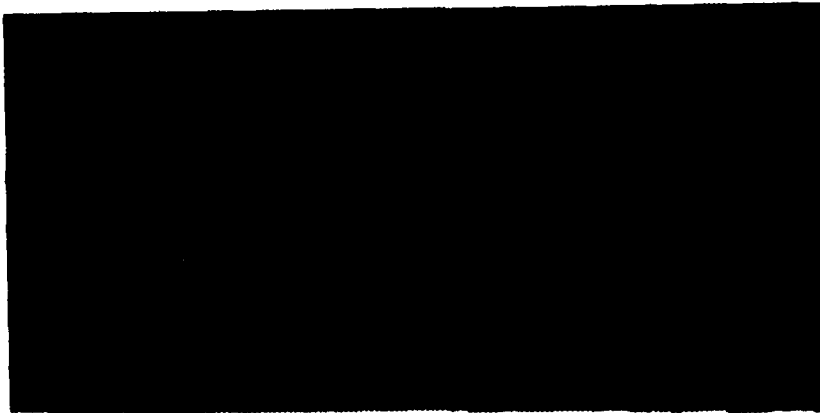


Fig. A-13: Impact side of Specimen A9, 11.69 ft-lbs (15.8 J).



Fig. A-14: Back Side of Specimen A9, 11.69 ft-lbs (15.8 J).



Fig. A-15: Impact Side of Specimen A10, 11.7 ft-lbs (15.9 J).



Fig. A-16: Back Side of Specimen A10, 11.7 ft-lbs (15.9 J).

A.2. "C" Scans of Damage Areas

order of 100 microns for the 2.35 ft-lb impact. The 100 microns is the resolution of the scan.

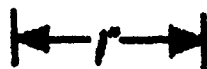


Fig. A-17: "C" Scan of Specimen A3, 2.35 ft-lb Impact.

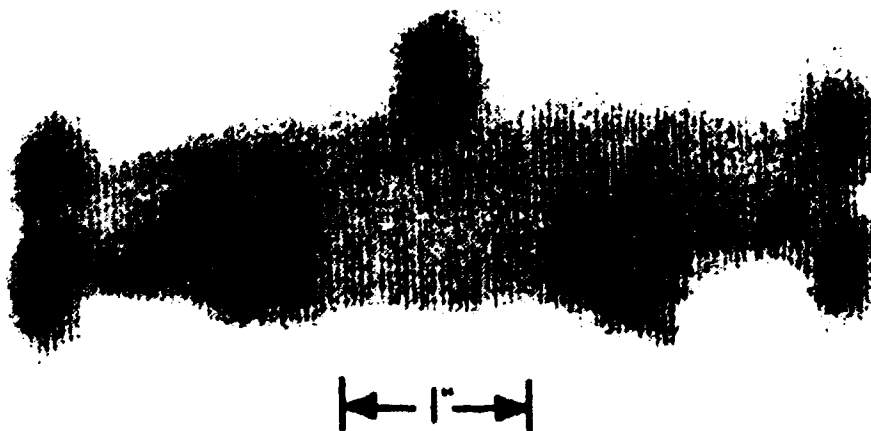


Fig. A-18: "C" Scan of Specimen A3 After Compression Loading.

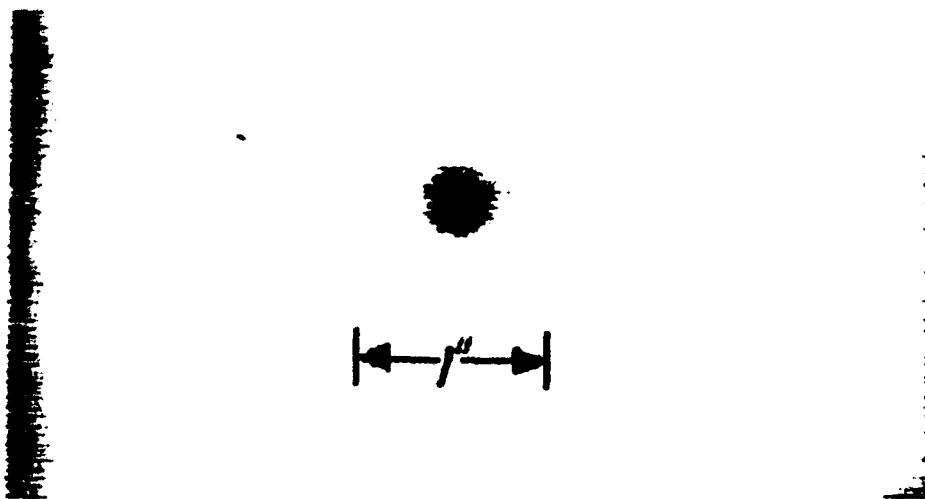


Fig. A-19: "C" Scan of Specimen A4, 2.39 ft-lb Impact.

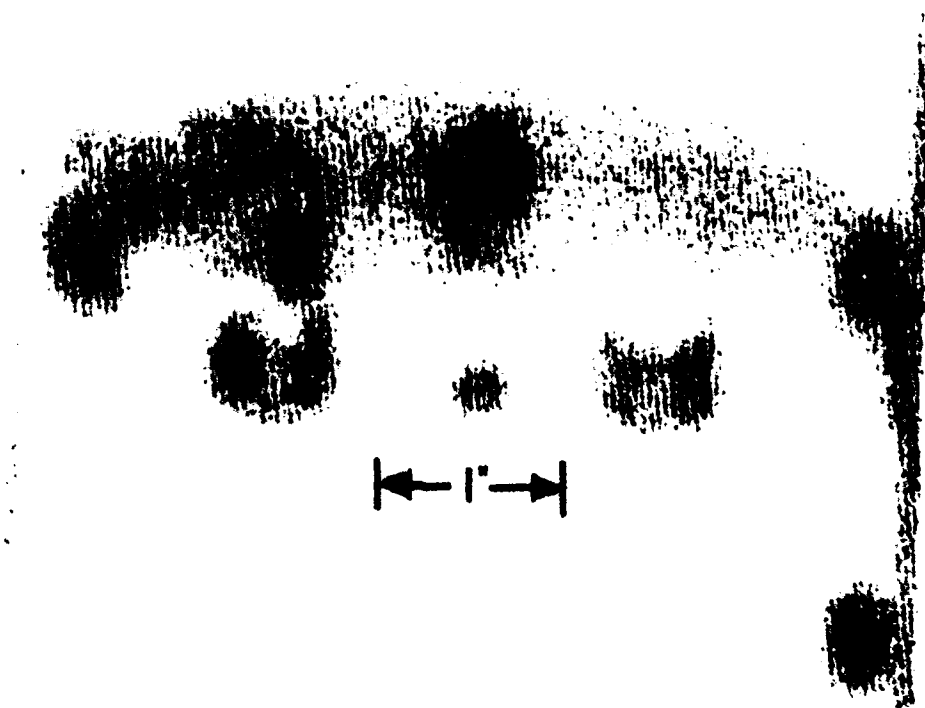


Fig. A-20: "C" Scan of Specimen A4 After Compression Loading.

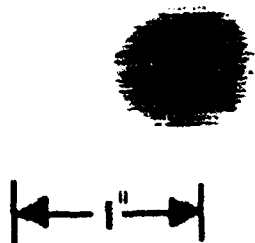


Fig. A-21: "C" Scan of Specimen A5, 5.54 ft-lb Impact.

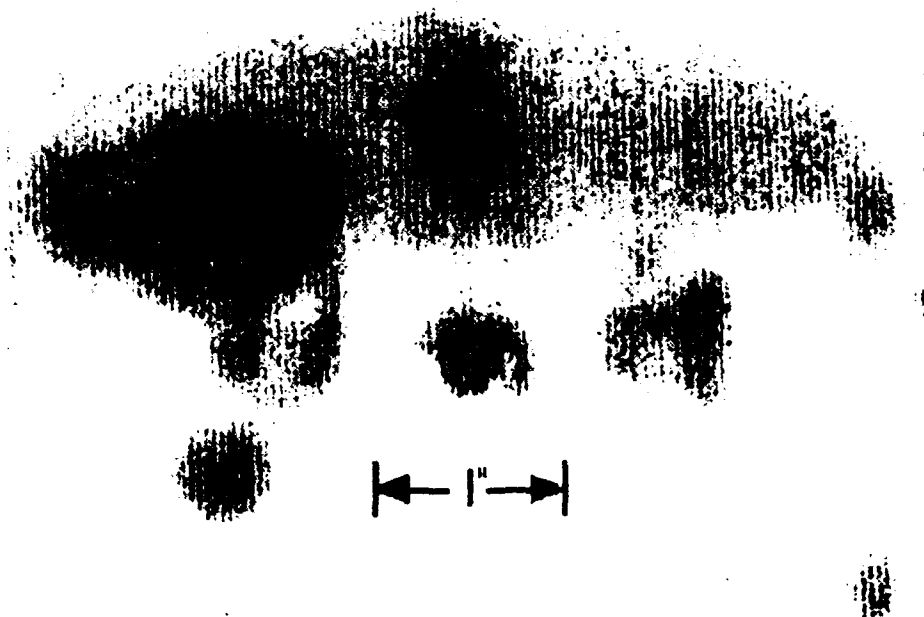


Fig. A-22: "C" Scan of Specimen A5 After Compression Loading.

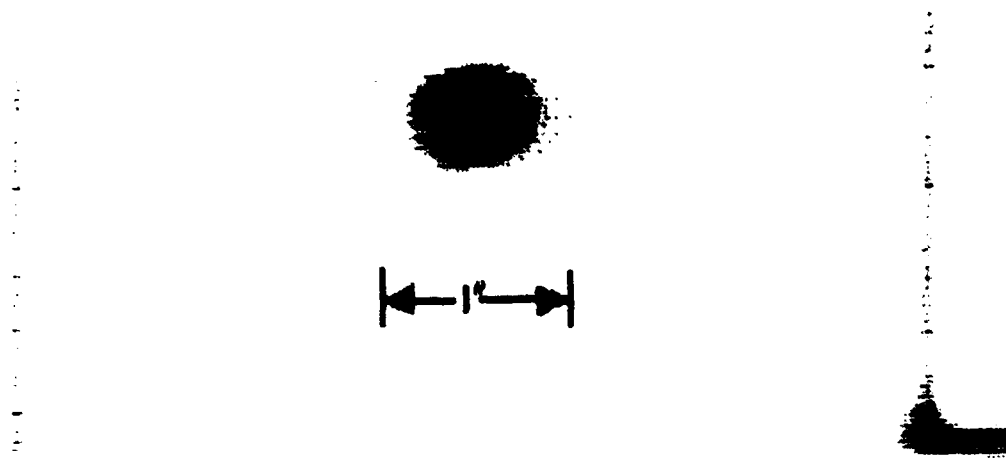


Fig. A-23: "C" Scan of Specimen A6, 5.49 ft-lb Impact.

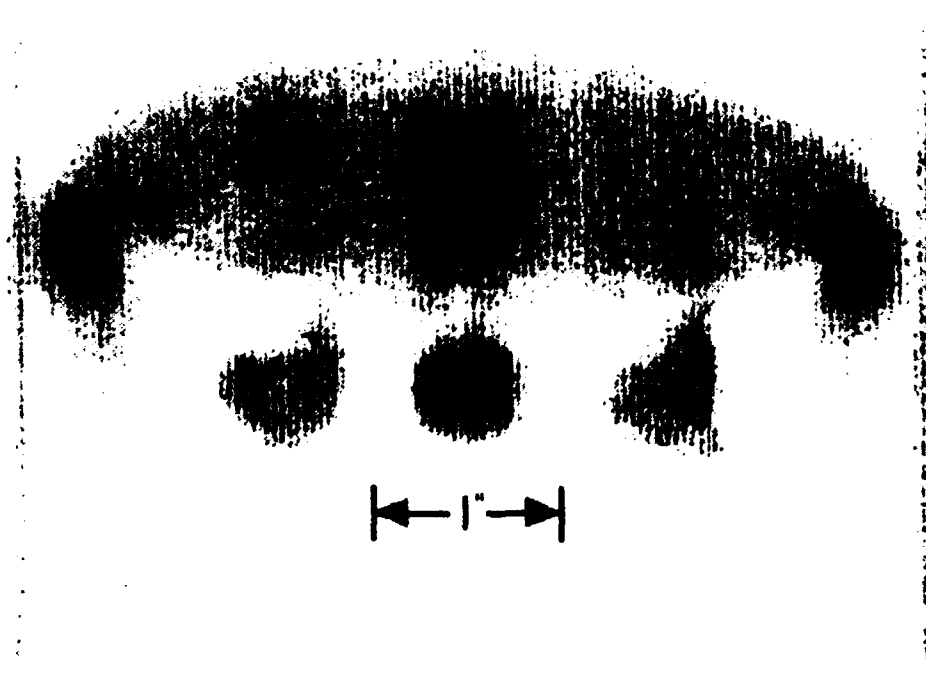


Fig. A-24: "C" Scan of Specimen A6 After Compression Loading.

4-10-80 11:11 AM 10.45 FT-LB IMPACT



Fig. A-25: "C" Scan of Specimen A7, 10.45 ft-lb Impact.

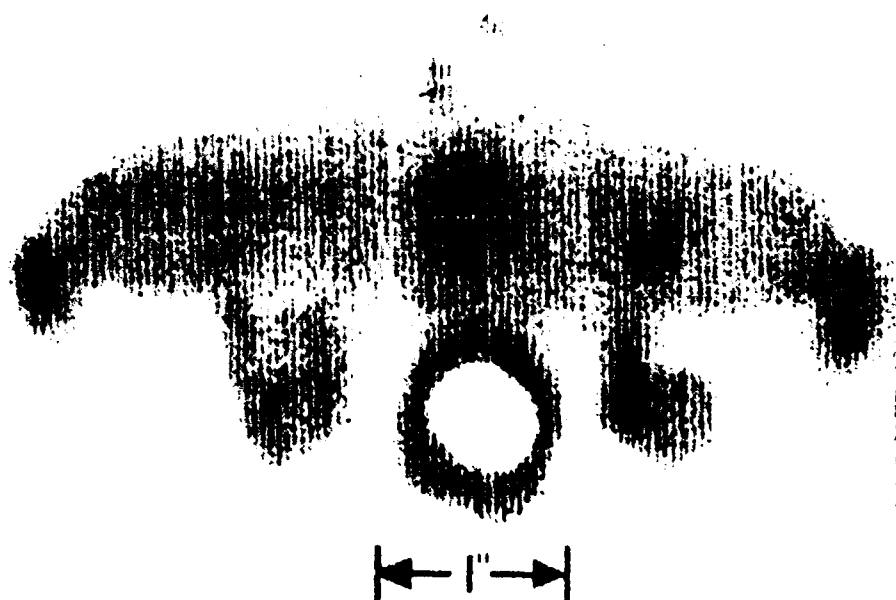


Fig. A-26: "C" Scan of Specimen A7 After Compression Loading.

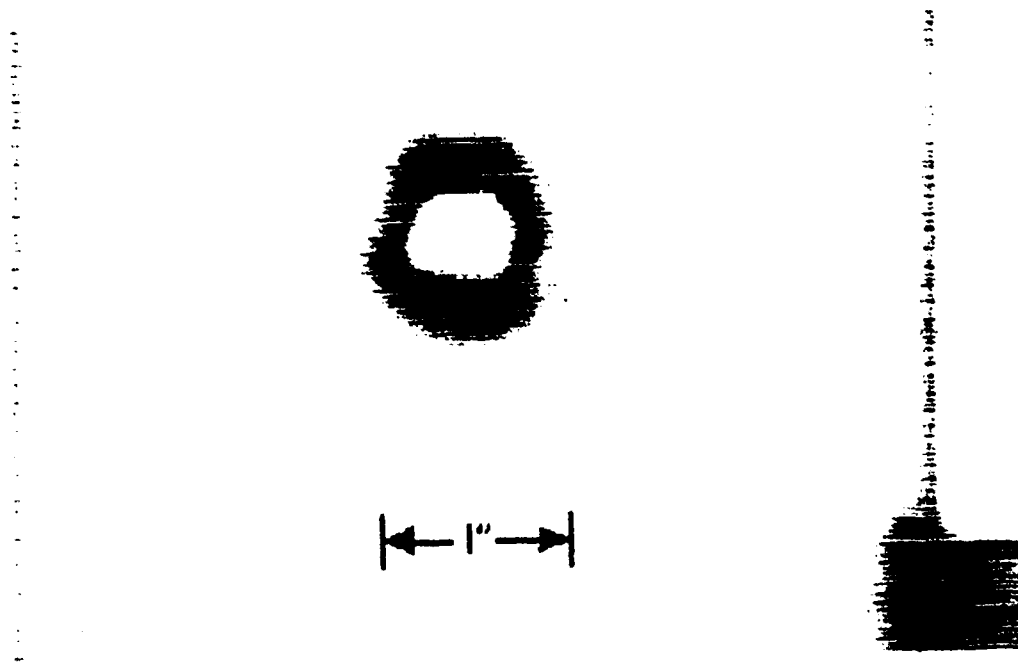


Fig. A-27: "C" Scan of Specimen A8, 10.31 ft-lb Impact.

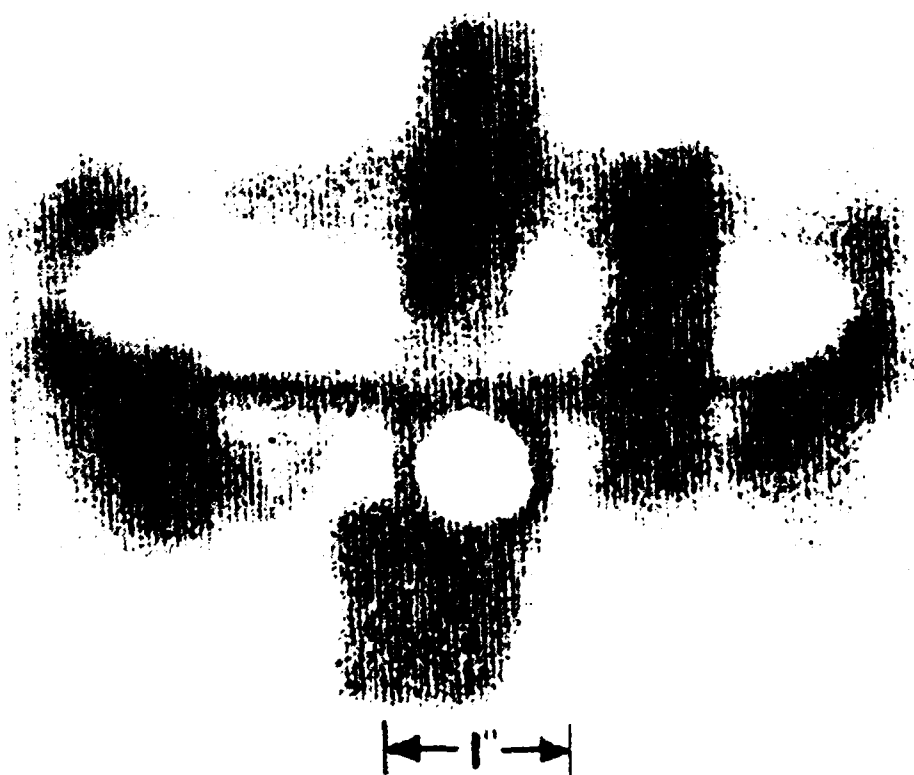


Fig. A-28: "C" Scan of Specimen A8 After Compression Loading.

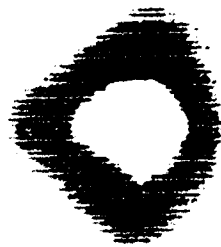


Fig. A-29: "C" Scan of Specimen A9, 11.69 ft-lb Impact.



Fig. A-30: "C" Scan of Specimen A9 After Compression Loading.

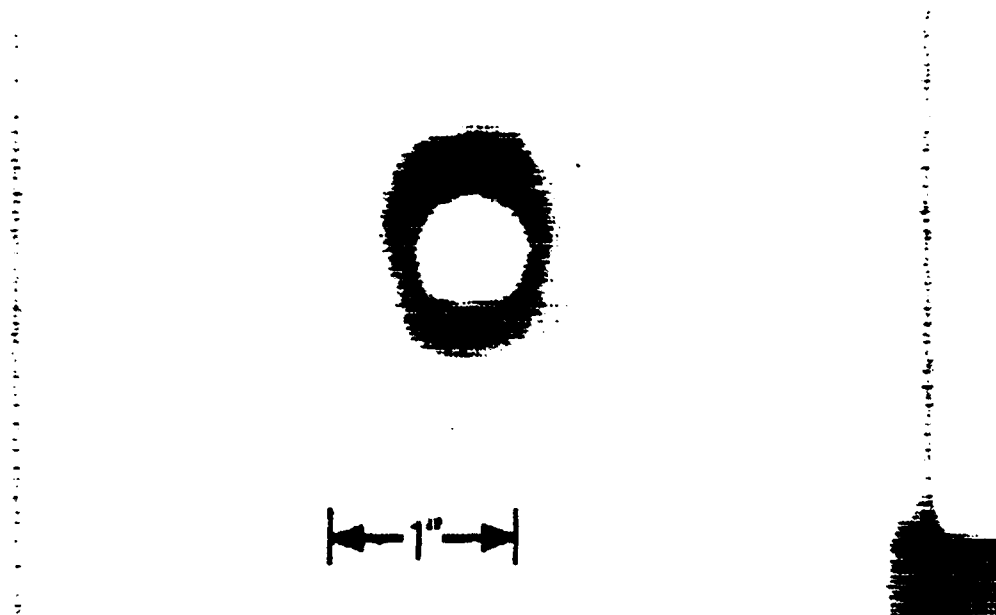


Fig. A-31: "C" Scan of Specimen A10, 11.7 ft-lb Impact.

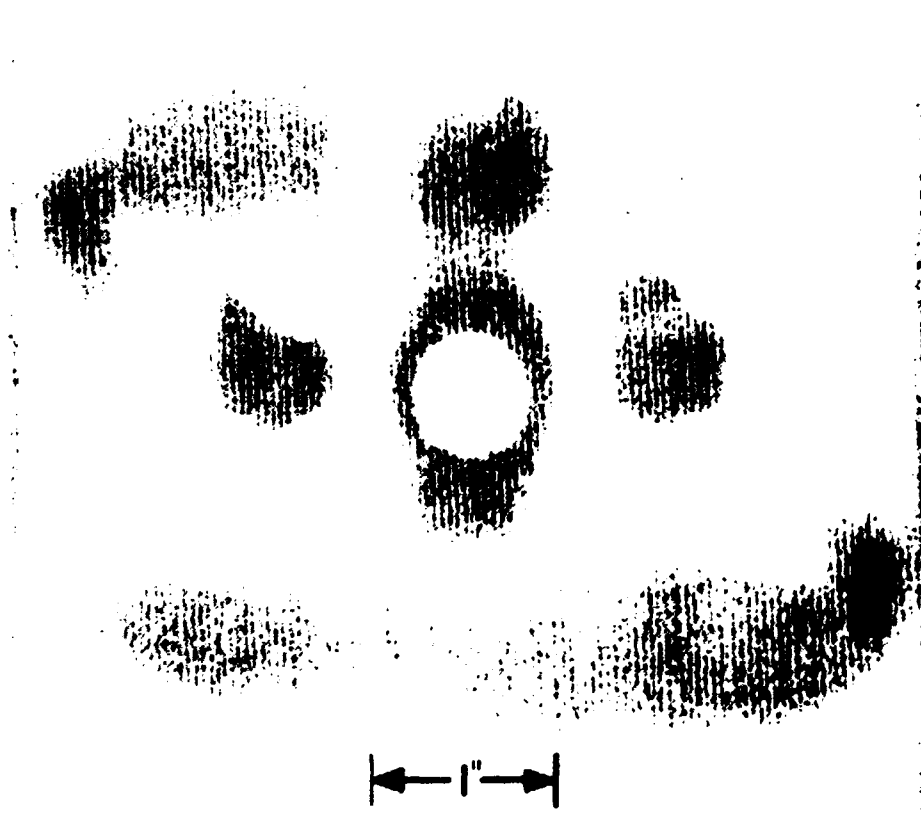


Fig. A-32: "C" Scan of Specimen A10 After Compression Loading.